

NUMERICAL SIMULATION AND DEVELOPMENT OF A
FERROFLUID PUMPING DEVICE DRIVEN BY
ELECTROMAGNETS

By

Otoniel Veléz Reyes

A thesis submitted in partial fulfillment of the requirements for the degree of

MASTER OF SCIENCE

in

MECHANICAL ENGINEERING

UNIVERSITY OF PUERTO RICO
MAYAGÜEZ CAMPUS

December, 2009

Approved by:

Stefano Lionardi, Ph.D
Member, Graduate Committee

Date

Oscar Perales, Ph.D
Member, Graduate Committee

Date

Gustavo Gutierrez, Ph.D
President, Graduate Committee

Date

Paul Castillo, Ph.D
Representative of Graduate Studies

Date

Gustavo Gutierrez, Ph.D
Chairperson of the Department

Date

Abstract of Dissertation Presented to the Graduate School
of the University of Puerto Rico in Partial Fulfillment of the
Requirements for the Degree of Master of Science

**NUMERICAL SIMULATION AND DEVELOPMENT OF A
FERROFLUID PUMPING DEVICE DRIVEN BY
ELECTROMAGNETS**

By

Otoniel Veléz Reyes

December 2009

Chair: Gustavo Gutierrez

Major Department: Mechanical Engineering

ABSTRACT

This thesis present a development of an Electromagnet Pumping Device (EPD) using a ferrofluid. A moving magnetic field is used as a driving force. A loop is set up with a series of solenoids which operate sequentially to generate a moving magnetic field. The system will be controlled by an electronic circuit to achieve the sequence required to operate the electromagnets. This non conventional pump has no moving parts other than the ferrofluid and thus, it has great potentials in variety of branches of engineering. The working fluid for the system is $Mn_{0.5}Zn_{0.5}Fe_2O_4$. A numerical simulation were carried out to evaluate and select the proper time step for each coil afterwards. A prototype was fabricated to prove the concept.

Resumen de Disertación Presentado a Escuela Graduada
de la Universidad de Puerto Rico como requisito parcial de los
Requerimientos para el grado de Maestría en Ciencias

**SIMULACION NUMERICA Y DESARROLLO DE UNA BOMBA DE
FERROFLUIDOS ACCIONADA POR ELECTROIMANES**

Por

Otoniel Veléz Reyes

Diciembre 2009

Consejero: Gustavo Gutierrez
Departamento: Ingeniería Mecánica

RESUMEN

Esta tesis presenta el desarrollo de un dispositivo de bombeo usando electroimanes (EPD), la cual produce movimiento de un ferrofluido debido a un campo magnético móvil. Un lazo es configurado con una serie de solenoides que operan de forma secuencial a fin de generar un campo magnético móvil en torno al lazo. El sistema es controlado por un circuito electrónico que realiza la secuencia requerida para operar los electroimanes. Esta bomba es diseñada sin ninguna parte móvil, mas que el fluido mismo, por tanto, podría tener una gran variedad de aplicaciones potenciales en ingeniería. El fluido de trabajo para el sistema es $Mn_{0.5}Zn_{0.5}Fe_2O_4$. Simulaciones numéricas fueron realizadas para evaluar y seleccionar el paso del tiempo apropiado para cada bobina. Luego, se construyó un prototipo para probar el concepto.

Copyright © 2009

by

Otoniel Veléz Reyes

To my daughter Camila for being my inspiration and my biggest treasure. To my mother Martha and my father Salvador (Reyno), for inculcating in me the moral values and principles that have made me the man I am, for all your advice and the great education that you gave me this work and its fruits are for you. To my sisters Fioldaliza, Kenia and my brothers Manuel and Jorge you were a motivating force for me to give my best on this academic challenge of my life. To Yakan for taking care of my daughter during my studies and being the best mother I wanted give to my daughter. To my cousins, nephews, nieces, uncles and my grandma Prieta thank you all for your love. To my friends Marcos, Roberto, Raul, Gabriel, Felipe and my roommate Carlos Thanks for being all my strength and inspiration in this project, thank you very much guys.

ACKNOWLEDGMENTS

I would like to thank my advisor Dr. Gustavo Gutierrez for all his honest and sincere counseling, help and commitment, and above all for believing in me. I am also very grateful to Dr. Ramón Vázquez Espinosa, Dean of Engineering, for his support, advice and above all for his friendship. To Oscar Perales and his nanomaterials group for his help and disposition, especially for his advice in the materials science area. To Stefano Leonardi for his help and good nature. I am grateful to the Mechanical Engineering Department and to the DoD-HBCU program for their financial support. To Miguel Riccetti, for all your unconditional help and to be a key part in the accomplishment of my goals . To Jose Villalobos, Javier, Andres, Christian, Edgardo and Josue for their selfless help in this work.

Finally, I specially thank to my friends for their support and all the memories.

TABLE OF CONTENTS

	<u>page</u>
ABSTRACT ENGLISH	ii
ABSTRACT SPANISH	iii
ACKNOWLEDGMENTS	vi
LIST OF TABLES	viii
LIST OF FIGURES	ix
LIST OF SYMBOLS	x
1 INTRODUCTION	1
1.1 Motivation	3
1.2 Objectives	4
2 LITERATURE REVIEW	5
2.1 Background	5
2.1.1 Magnetism	5
2.1.2 Magnetic materials	6
2.1.3 Ferrofluids	8
2.1.4 Solenoid	10
2.2 Review of magnetic pumping devices using ferrofluid	11
2.3 Contribution of this research	19
3 MATHEMATICAL FORMULATION	21
3.1 Magnetostatic Relations	22
3.2 Ferrofluid flow formulation	28
3.3 Solver package	29
3.4 Proposed numerical model	30
3.5 Boundaries conditions	31
3.5.1 Boundaries conditions for the magnetostatic field	31
3.5.2 Boundary conditions for Navier Stokes equations	31
4 METHODOLOGY	32
4.1 Operation	33
4.2 Working fluid	34
4.3 Coil design	35

4.4	Control unit	37
4.5	Design parameters of the device	37
5	RESULTS	38
5.1	Results of the design of the solenoid	38
5.2	Results of the numerical simulation	40
5.3	Results of the characterization	42
6	CONCLUSIONS AND RECOMMENDATIONS	47
A	INTRODUCTION TO ELECTROMAGNET DESIGN	49
A.1	Maxwell Equations	49
A.2	Generation of static magnetic field	50
A.3	Magnetic properties of core materials	51
A.4	Remanent field	53
A.5	Eddy current effects	54
A.6	Connection of coil in derivation	54
A.7	Field measurement	57
B	CONTROL CIRCUIT FOR ELECTROMAGNET PUMPING DEVICE	58
B.1	Control unit	58
	B.1.1 Components	58
	REFERENCES	62

LIST OF TABLES

<u>Table</u>		<u>page</u>
2-1	Comparison of different ferrofluids in a magnetocaloric pump	12
4-1	a) Coil data, see figure 4-4; b) Wire data are (These parameters were used to build the solenoids)	36
4-2	Summary of the solenoids design parameters	36
4-3	Materials to develop the electromagnet pumping device	37
5-1	Current density for different voltage applied in the model designed . . .	41

LIST OF FIGURES

Figure	page
1-1 Device prototype, arrangement of the solenoids around the loop	2
1-2 Sectional view of the coil wrapping the pipe	2
2-1 Electron motion in an orbit	6
2-2 Magnetic dipole orientation for different materials	8
2-3 Magnetic behavior and hysteresis loop for different materials	9
2-4 Schematic Ferrofluid composition	9
2-5 HRTEM images of $Mn_{0.7}Zn_{0.3}Fe_2O_4$ nanocrystals at different magnifications.	10
2-6 Magnetic field produced by electric current in a solenoid coil, similar to magnetic field produced by a magnet bar	11
2-7 a.Schematic diagram of a miniature automatic cooling device. b.Distribution of the magnetic field.	13
2-8 Simulated temperature distribution of the magnetic fluid in presence of a specific magnet location.	14
2-9 Concept of the stepper micropump (a) the pump chip with the circular channel (b) the stator with eight solenoids (c) control scheme for solenoids.	15
2-10 Angular displacement(a) and angular velocity (b) of the stepper micropump	16
2-11 3D geometry of blood vessel	17
2-12 Fluid velocity field with magnetic flux density	18
2-13 Experimental setup achieved by Kraub	18
2-14 Maximal velocity measure as function of the field amplitude	19
3-1 A magnetic dipole in a magnetic field B	22
3-2 Magnetization-Magnetic field curve for different temperature	28

3-3	Model view in the COMSOL window	30
4-1	Electromagnet pump device	33
4-2	Time sequence for the operation of the solenoids	34
4-3	Distribution of coils along the ferrofluid loop	35
4-4	Cross section view of a solenoid to be wrapped on the loop	35
5-1	Numerical model and magnetic field in a coil	40
5-2	Magnetic field generated by the time function in the solenoids	43
5-3	Velocity profile for the model	44
5-4	Flow velocity for 24V, 48V and 110V solenoids input voltage	44
5-5	Solenoid view	45
5-6	Solenoids wrapped around the loop	45
5-7	Electromagnets ferrofluid pump prototype	46
A-1	B-H curve which describes materials magnetic properties	52
A-2	Toroidal electromagnet with gap	54
A-3	Derivation coil connected	55
B-1	PIC16F84A Microcontroller	58
B-2	Optoisolator 4N25	59
B-3	Power MOSFET IRF520NPbF	59
B-4	Schematic control circuit to supply sequenced power to solenoids	60
B-5	Control unit circuit to supply sequenced power to solenoids	61

LIST OF SYMBOLS

t	Time (seconds)
A	Ampere.
B	Magnetic flux density
\mathbf{F}	Magnetic body force
Fe	Iron
g	Gravity acceleration
\mathbf{H}	Applied magnetic field
H_c	Coercitivity
J	Joule
J_f	Electric current density
K	Kelvin degree
Kg	Kilogram
m	Meter
\mathbf{M}	Magnetization
EPD	Electromagnet pumping device
MLCD	Magnetic Cooling Loop Device
\mathbf{M}_r	Remanence Magnetization
Mn	Manganese
\mathbf{M}_{ff}	Ferrofluid magnetization
\mathbf{M}_s	Saturation Magnetization

Na	Sodium
O	Oxygen
P	Dynamic pressure
P_{mag}	Magnetic pressure
P_T	Total pressure
Pa	Pascal
q	Heat flux
Re	Reynolds number
T	Temperature, Tesla
T_C	Curie temperature
T_D	Demagnetization temperature
\bar{v}	Mean velocity
\mathbf{v}	Velocity
V	Volume, voltage
VSM	Vibrating sample magnetometer
W	Watts
Zn	Zinc
χ	Magnetic susceptibility
ϕ	Volume fraction
ψ	Scalar potential
η	Dynamic viscosity
μ_0	Permeability of the free space
μ_r	Relative permeability

ρ	Density, resistivity
\mathbf{f}	Force over a moving charge
Q	Charge
∇	Vector differential operator
N_{turs}	Number of turn of a coil
R_A	coil radial length
d_c	Conductor diameter with coating
$N_{turns/layer}$	Number of turns per layer of coil
ϵ	Electric permeability
I	Current
R	Resistance
Θ	Ampere-turns
S_c	Conductor transversal area
δ	Current density

CHAPTER 1

INTRODUCTION

In this section a Magnetic Cooling Loop Device (MCLD) with no moving parts. In general, pumping device for ferrofluid can be classified in two categories, the mechanical and the non mechanical. Most of the mechanical ones are magnetocaloric pump which generate the fluid motion by magnetocaloric effect [1–3] and membranes pump, which exert the force over the fluid by alternating moving of the membranes. Different principles for actuation of the pump can be mentioned, as thermoneumatic [4], electrostatic [5], pneumatic [6] and piezoelectric actuation [7]. The major advantage of the above mentioned pumps is the less limitation on the properties of the operational liquid. However, these type of pumps require continuous maintenance program, high voltage and effectively usage in order to activate the membranes in practice.

Different to mechanical pumps, non mechanical pumps have been designed without any moving part and thus not suffered from wear nor fatigue problems caused by high pressure drop across the check valve. There are many non mechanical ferrofluid pumping device been demonstrated as diffuser/nozzle pumps [8], electro-dynamics pump [9], magneto-hydrodynamics [10], magnetocaloric pump [2, 3] and electro-kinetic pumps [11].

A new pumping concept using a ferrofluid is proposed. A magnetic fluid will flow through a loop, moved by magnetic force exerted by a series of solenoids distributed around it. Solenoids will turn on sequentially controlled by a power electronic circuit. Since no mechanical moving parts are present in the device, other than ferrofluid,

it has great potentials in a variety of branches of thermal engineering applications. The core of the solenoids will be wrapped in the pipe of the loop, in this way the ferrofluid permeability will increase the magnetic field at the center of it. As shown in fig 1-1 prototype was developed with five similar coils around the loop. Fig. 2-6 represent a sectional view of one of this coils.



Figure 1-1: Device prototype, arrangement of the solenoids around the loop

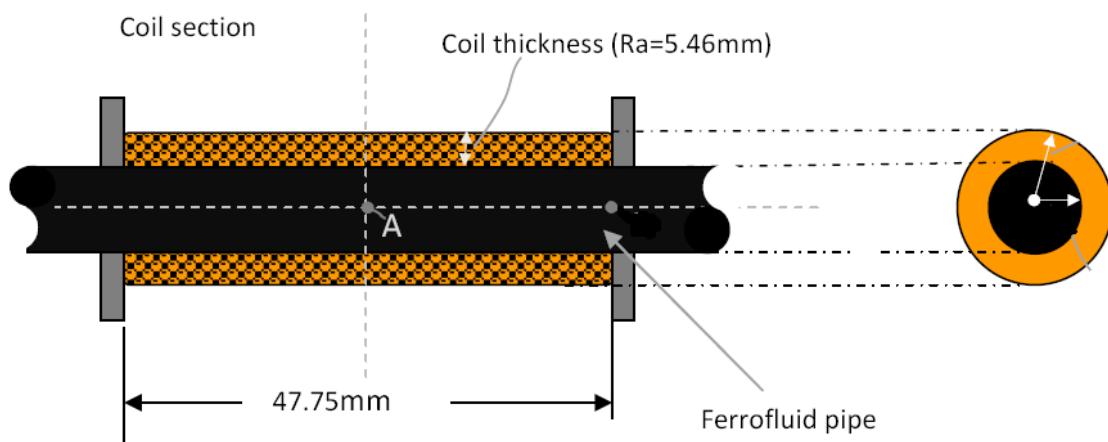


Figure 1-2: Sectional view of the coil wrapping the pipe

1.1 Motivation

In the proposed device a pressure gradient in a ferrofluid is generated by the effect of a moving magnetic field in the loop. The magnetic field is generated by an arrangement of solenoids around the loop. Power is sequenced in order to transport the magnetic field through out the loop. Application of this device configuration can be used in cooling loop system in which maintenance and vibrations are an issue and has to be reduced .

Ferrofluids are a key component of the proposed device. This substance is colloidal fluids consisting of magnetic nanosize particles (10-50nm) suspended in water base or oil base, called carrier substance [12–14]. Volume proportion of particles in carrier fluids are about 4-5 %. The proposed pumping system uses Mn-Zn ferrite as a working ferrofluid in an array of elements. These elements are: the electromagnet, the solenoids which generate the moving magnetic field; sequencer device, electronic circuit capable to sequence the power of the electromagnets.

This refrigeration circuit is attractive for electronic cooling for example where maintenance is minimized due to the absence of moving parts. Numerical modeling and experimental development of this loop will be carried out in this work.

1.2 Objectives

Develop numerical model of a device for magnetic fluid transport. Design and develop prototype to evaluate operational parameters of the device. The following tasks will be executed for carrying out this goal.

- a) Design a group of solenoids to generate a moving magnetic field around a loop
- b) Conduct a series of numerical simulation of the proposed concept to define the optimal operative parameters to elaborate the device.
- c) Construct the ferrofluid loop and solenoids to be distributed around it.
- d) Design and construct of an electronic circuit to control the operation of the solenoids.
- e) Conducting a series of experiments to define the operation of an electromagnetic pumping device.

CHAPTER 2

LITERATURE REVIEW

2.1 Background

In this section, a brief review of the magnetic behavior of materials, the generation of magnetic fields and the magnetic fluids is presented

2.1.1 Magnetism

The term magnetism is used to describe how materials respond on the microscopic level to an applied magnetic field. It is a phenomenon through which materials exert an attractive or repulsive force on other materials. The contribution to net magnetic moment is originated principally by two sources: one is related to the orbital motion and the other one is attributed to the spin motion. The Bohr theory of magnetism states that an electron which orbits around the nucleus of an atom originates the magnetic behavior of matter. An electron is defined as a small current loop producing a quite little magnetic field having magnetic moment along its rotation axis. Fig. 2-1 show schematically this model. Later, in 1925 Goudsmit and Uhlenbek [15] introduced the concept of electron spin, which better explains the origin of magnetism. Spin is the movement of the electron around its axis, which also contributes to the magnetic moment in the atom.

One of the fundamental concepts in magnetism is the magnetic field. A magnetic field is generated in a volume of space when there is a change in magnetic energy of that volume. The force produced by the magnetic energy gradient can be detected by the acceleration of an electric charge moving in the field by the force

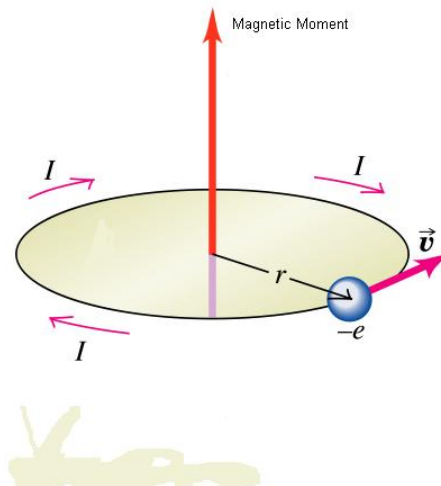


Figure 2-1: Electron motion in an orbit

on a current-carrying conductor, or by the torque on a magnetic dipole [16]. All magnetic phenomena are produced due to electric moving charges [17].

Since a magnet bar gets its ferromagnetism from electrons distributed evenly throughout the bar, when a magnet bar is cut in half, each of the resulting pieces are smaller magnet bar. Even though a magnet is said to have a north pole and a south pole, these two poles cannot be separated from each other. Essentially, it says that there is no such thing as a magnetic monopole. [18]

2.1.2 Magnetic materials

The combination of all the moments of a material determines the magnetization of the material [19]. For an isolated current loop or magnetic dipole, the field of the loop itself always acts to add to the external field giving an increased field in the neighborhood of the loop. All the moments can influence the field upon its arrangement. Some classes of magnetic materials are diamagnetic, paramagnetic, ferromagnetic, ferrimagnetic and superparamagnetic. A briefly description presented on next.

1. In *diamagnetic* materials, (as bismuth) the spin moments are generally dominant and the field generated is opposite to the external field. Thus, the internal

magnetic field is reduced slightly compared to the external field. Fig.B-3(a) show schematically this behavior.

2. In *paramagnetic* materials (as Tungsten) the dipole moments dominate slightly. This makes the external field be increased slightly. This type of behavior is schematically presented in fig.2-2(b).
3. In *ferromagnetic* material, (as iron) large dipole moments are produced in certain domains. For native or virgin ferromagnetic material, when an external field is applied and then removed, a net alignment occurs giving a permanent magnetization. Alloys of some of the ferromagnetic materials are also ferromagnetic (Alnico). See figure 2-2(c)
4. In *ferrimagnetic* materials, adjacent atoms develop unequal, but oppositely directed moments, allowing a rather larger response to external fields. From the point of view of engineering applications, the ferrites are very important ferrimagnetic materials. Ferrites possess a very high resistance, and hence give very little eddy current loss at higher frequencies when used as transformer core. For illustration see figure 2-2(d)
5. In *superparamagnetic* behavior, (as presented in ferrofluids). The thermal energy is sufficient to change the direction of magnetization of the entire crystallite. The resulting fluctuations in the direction of magnetization cause the magnetic field to average to zero. Thus the material behaves in a manner similar to paramagnetism, except that instead of each individual atom being independently influenced by an external magnetic field, the magnetic moment of the entire crystallite tends to align with the magnetic field.

Induced magnetic flux density (\mathbf{B}) and the magnetizing force (\mathbf{H}) are related by the hysteresis loop, often referred as the $\mathbf{B-H}$. Magnetization curves describes the magnetic behavior of materials. H_c is the *coercivity* which is the magnetic field

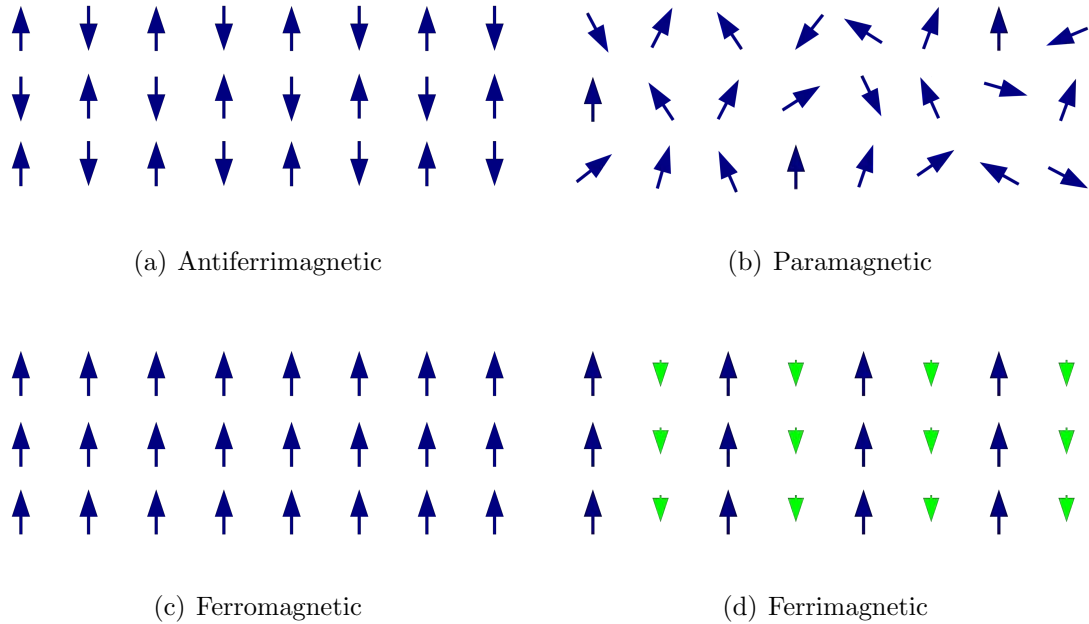


Figure 2–2: Magnetic dipole orientation for different materials

required to demagnetize the material. M_s is the saturation magnetization, defined as the state reached when an increase applied to external magnetic field do not produce an increase in the magnetization of the material. In this situation, all the magnetic dipoles are oriented in the same direction of the applied field. Figure 2–3 shows the hysteresis loop for different types of materials [20]. Magnetic susceptibility (χ) is the strength of the response to an induced magnetic field $\frac{\partial M}{\partial H}$. Remanence M_r is the magnetization remaining after an external magnetic field is removed.

2.1.3 Ferrofluids

Ferrofluids or magnetic fluids are stable colloidal suspensions of magnetic particles dispersed in a liquid carrier. Particle sizes generally range from 5 to 30 nm and the volumetric loading from 1% to 5%. In a stable magnetic fluid the size of the magnetic particles must be well controlled not only to tune the magnetic behavior within the single domain limits but also to keep non-agglomerated particles in suspension even during exposure to strong magnetic fields. Particles agglomeration and

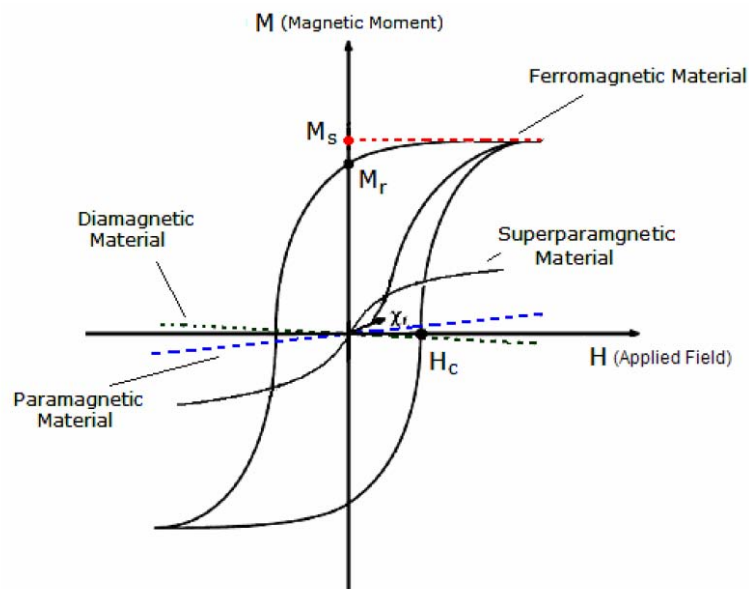


Figure 2-3: Magnetic behavior and hysteresis loop for different materials subsequent settling can be avoided by using a surfactant or other type of coating [1]. The coating agent must be matched to the carrier type and it must overcome the Van der Waals and magnetic forces in order to prevent agglomeration and further precipitation of the nanoparticles. A schematic of a ferrofluid composition is presented in figure 3.2. Figure 3.3 shows a nano nanocrystal ferrite from HRTEM [21]

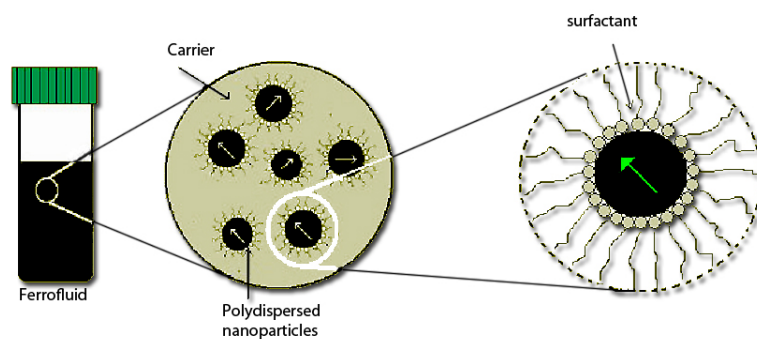


Figure 2-4: Schematic Ferrofluid composition

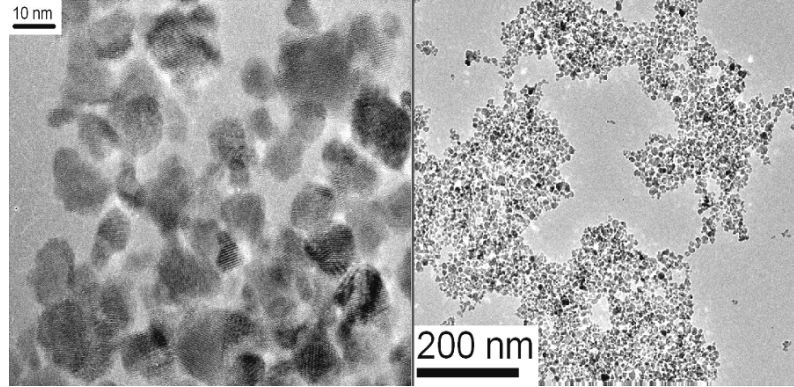


Figure 2–5: HRTEM images of $Mn_{0.7}Zn_{0.3}Fe_2O_4$ nanocrystals at different magnifications.

In a colloidal ferrofluid the particles behaves as the molecules of a paramagnetic gas, each with its embedded magnetic moment \mathbf{m} [13]. In the absence of an applied field, the particles are randomly oriented and the fluid has no net magnetization. However for ordinary field strengths the tendency of the dipole moments to align with the applied field is partially overcome by thermal agitation. When the field magnitude is increased, the particles tend to align more and more with the field direction. For very high field strengths the particles may be completely aligned getting the saturation magnetization value.

2.1.4 Solenoid

Solenoid is an electric device compounded of a three dimensional coil [22]. Solenoids refers to a loop or a group of loop of wire wrapped around an air or metallic core. When an electric current passes through the wire, a magnetic field is generated in the core. Magnetic field from a solenoid can be controlled. This is important due to its usage as electromagnets. Solenoids refer specifically to magnets designed to produce a uniform magnetic field inside a volume of space (where some experiment might be carried out).

Solenoid power depend mainly on the current required by the coil and on the coil resistance [23]. Heat released in the form of I^2R is the primary power sink, and

solenoids are therefore limited by the heat they can dissipate. Solenoids can operate in continuous or pulsed mode and the power depends on the mode of operation. Compared with a magnet bar a solenoid has two poles as well upon the direction of the current. Fig 2–6 show a schematic field line between the north and south pole .

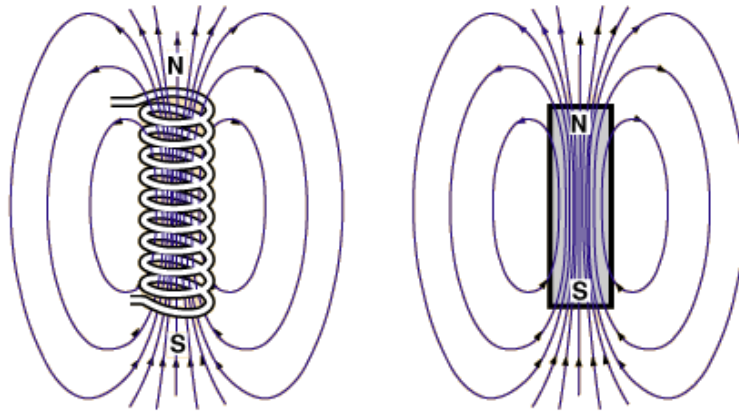


Figure 2–6: Magnetic field produced by electric current in a solenoid coil, similar to magnetic field produced by a magnet bar

2.2 Review of magnetic pumping devices using ferrofluid

Relevant works have been done by several authors in magnetic fluid pumping device. In this section, some important research in the area of magnetic energy conversion will be presented.

Magnetocaloric effect is the changing of a magnetic material temperature under magnetization in adiabatic conditions [13]. This effect was discovered by Warburg [24], and used by [1–3, 25] in magnetocaloric pump for ferrofluids. In this concept the ferrofluid loss its magnetization when is heated reaching again the magnetization when temperature decrease below the demagnetization temperature. This effect induce the fluid to move from high temperature to low temperature zone.

Rosensweig[13] proposed a direct and efficient conversion of heat in useful work with no mechanical moving parts. A magnetic material was postulated that could

flow through tubes and around bends and change its shape. On that base the magnetic fluid, suitable to transfer energy, seen justified.

Love et al.[1] developed a magnetocaloric pump for microfluidic applications using magnetic fluids with $Mn_{0.5}Zn_{0.5}Fe_2O_4$ nanoparticles suspended in water with average particle size between 6 and 20nm and a Curie temperature of approximately 150°C. Experiments were carried out with these ferrofluids, taking the magnetic field, heat input and temperature gradient as constant variables. In these experiments a 2-mm-diameter glass tube was used. The results showed a maximum velocity of 2.1 mm/s obtained for a temperature gradient of 13°C with a maximum temperature of 59°C for the water based ferrofluid. The velocity of the fluid was measured using a digital video camera and recording the displacement and time. Results were compared with calculated velocities using finite-element analysis. Table 2.2 shows a comparison for the different ferrofluids reported by Love et al.[1] The results for

Table 2–1: Comparison of different ferrofluids in a magnetocaloric pump

Ferro fluid	Spec. Grav.	Visc. (mPa.s)	Ms (mT)	T_{hi} (C)	V (mm/s)	Vfea (mm/s)
Fe3O4 in oil	1.40	375	35	86	0.23	0.17
Mn0.5Zn0.5Fe2O4 oil	1.52	380	25	61	1.6	1.59
Mn0.5Zn0.5Fe2O4 water	1.37	83	11	59	1.57	2.1

the measured velocity showed that for the ferrofluid with $Mn_{0.5}Zn_{0.5}Fe_2O_4$ particles suspended in water the velocity are in order of ten times higher than the ferrofluid with magnetite particles in oil. This result makes the MnZn ferrite ferrofluid a good candidate for magnetocaloric energy conversion.

Qiang Li,[3]. Developed a miniature devise consisting of Mn-Zn ferrite magnetic fluid loop, a permanent magnet, a heat source and heat sink. The loop is established

to validate the automatic cooling concept based on magnetocaloric effect principle. Schematic representation of this loop is shown in figure 2-7a. displaced to position A is indicated in figure 2-7b [3]

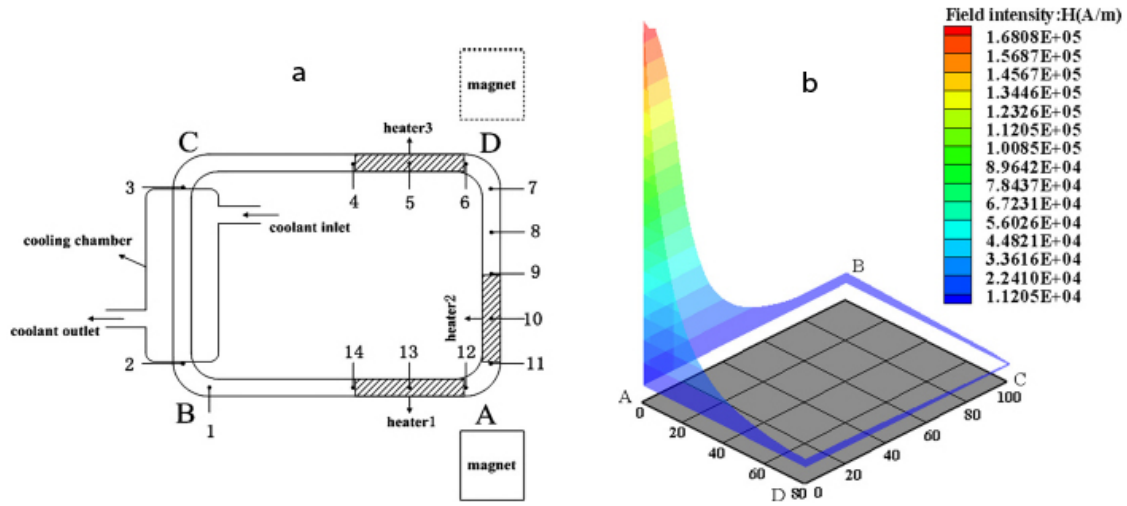


Figure 2-7: a.Schematic diagram of a miniature automatic cooling device. b.Distribution of the magnetic field.

Results show that there exist a non uniform temperature and magnetic fields inside the whole loop, the net magnetic driving force arises and the fluid circulates in the loop. Figure 4 indicates the effects of position and heat flux of the electric heater to find a suitable position for the heat source in the loop. From the temperature profiles shown in figure [3] one can learn that a heater at the position of heater 1 was put into operation, the magnetic fluid performed a clock wise flow.

The input load was 2.91w and the peak value of temperature of the ferrofluid just inlet of the heating section was 345.50K.

Nam-Trung [26] demonstrated a stepper micropump for ferrofluid driven system. The stepper micropump consists of two parts: the microchip and the external stator. Figure 2-9 show the stepper micropump and the control scheme for the solenoids [26].

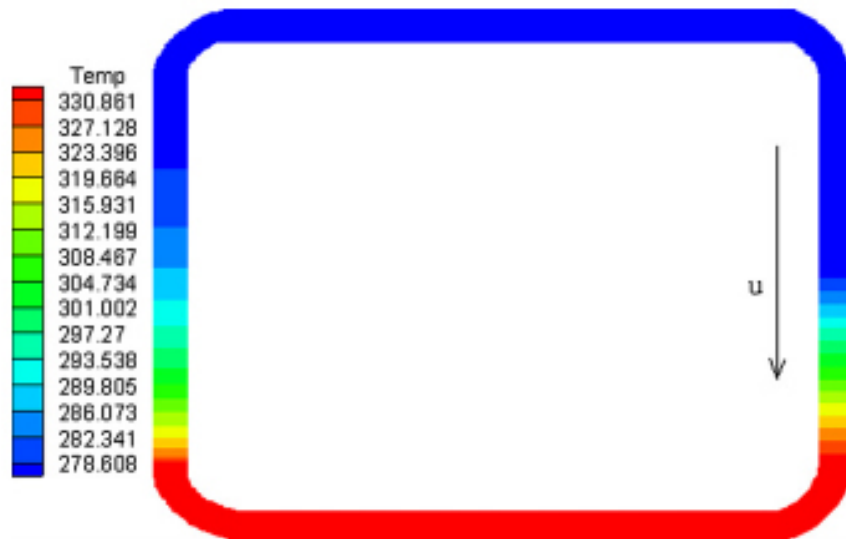


Figure 2–8: Simulated temperature distribution of the magnetic fluid in presence of a specific magnet location.

The stator is an array of eight solenoids arranged circularly around the channel loop. Fig. 2–9 shows the arrangement of these solenoids. The solenoids were modified from commercially available coils which have a resistance of 17.80.2 Ohms. The original core of the solenoid was replaced by a steel core of 6-mm diameter. The tip of the core was tapered to an angle of 20° to maximize the magnetic flux at the tip. The tapered cores were permanently attached to the solenoid using epoxy

The magnetic flux at the core tip was measured with a gaussmeter (GM05, Hirst Magnetic Instruments Ltd, UK). At a voltage of 20 V, the solenoid can induce a magnetic flux of approximately 250 mT. The trend shows that the magnetic flux at the core tip reaches its saturation value at about 20 V

Fig. 2–10 shows the magnetic flux at different voltages. At a voltage of 20 V, the solenoid can induce a magnetic flux of approximately 2,500 gauss. Saturation value for magnetic flux is reached at the core tip for a voltage value of 20V.

According to results experiments, activation period of each step and the driving voltage need to be optimized to synchronize the plug position with the positions of the actuating core tips. The sharp tip was used in order to bring high magnetic flux

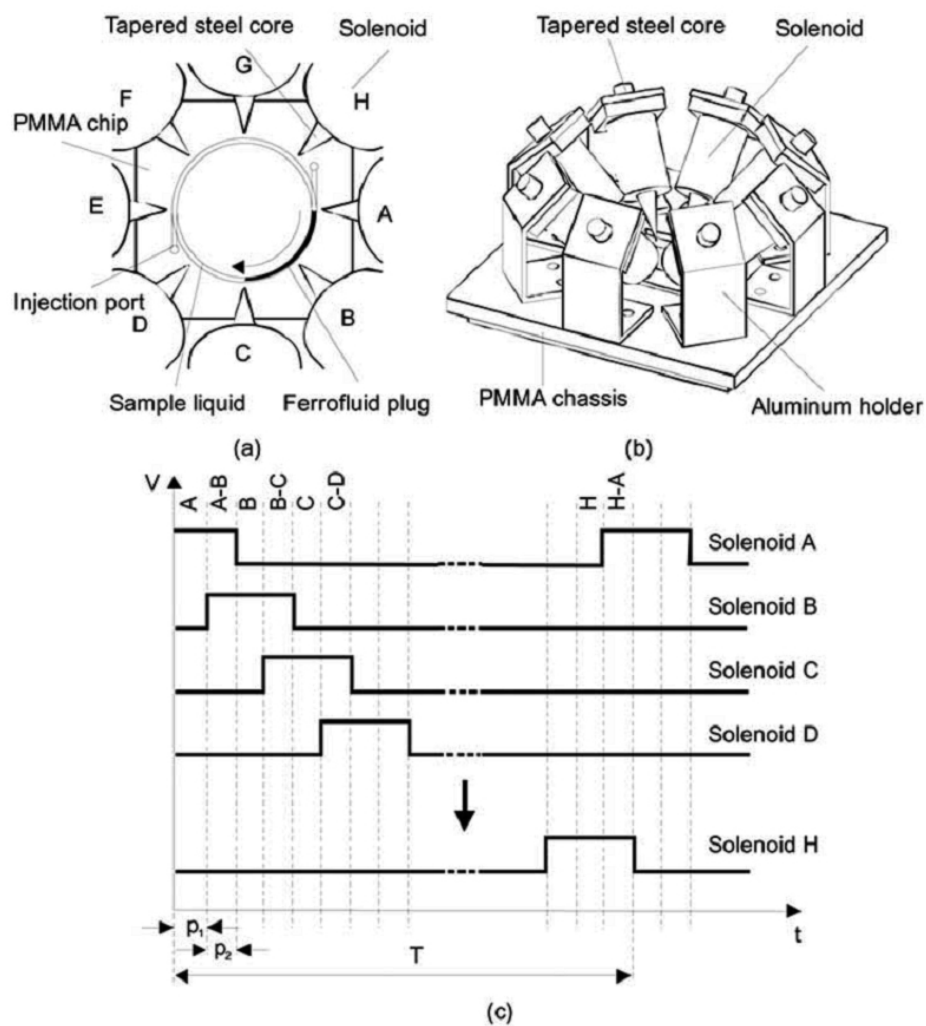


Figure 2-9: Concept of the stepper micropump (a) the pump chip with the circular channel (b) the stator with eight solenoids (c) control scheme for solenoids.

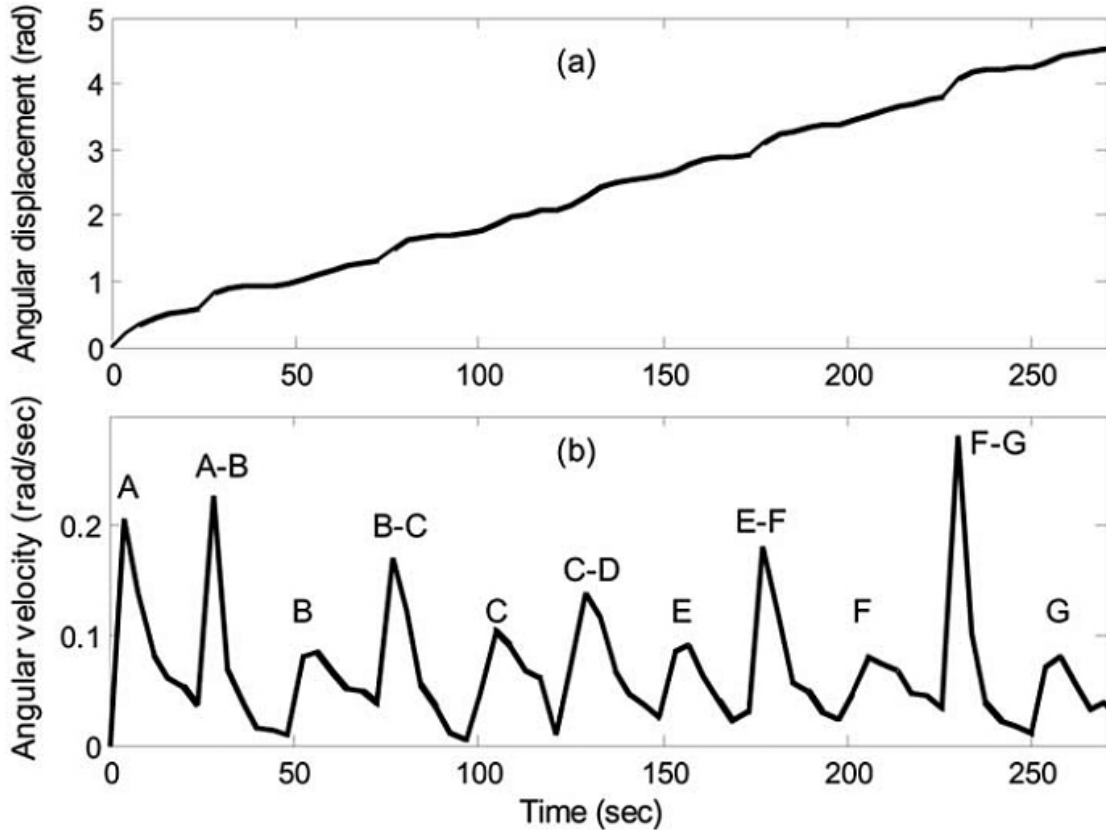


Figure 2–10: Angular displacement(a) and angular velocity (b) of the stepper micropump

and high field gradient. It was observed that at a high driving voltage and a short activation time, the ferrofluid tends to move faster on the channel wall, enclosing and forming silicone oil droplets inside it.

Lohakan, et al. [27] purposed a velocity field of magnetic fluid based on Partial Differential Equation (PDE). The development of this algorithm includes equation of conservation of mass and Navier-Stokes for dynamic fluid, and Maxwell's equations for magnetism. These nonlinear equations are analyzed by finite element method. The model is numerically computed in order to investigate the effect of magnetic potential vector with magnetic fluid flow in a transient model.

The magnetic vector potential generated by a magnet is calculated. The computed magnetic field generates a magnetic volume force that affects the flow field in the vessel analyzed. To describe the dynamic effects which produce fluid motion,

momentum equation and continuity equations were solved for an incompressible Newtonian flow.

A 3D model of blood vessel was constructed in order to observe the magnetic potential and fluid velocity field. It consists of blood vessel and magnetic device as is shown in figure 2-11 [27].

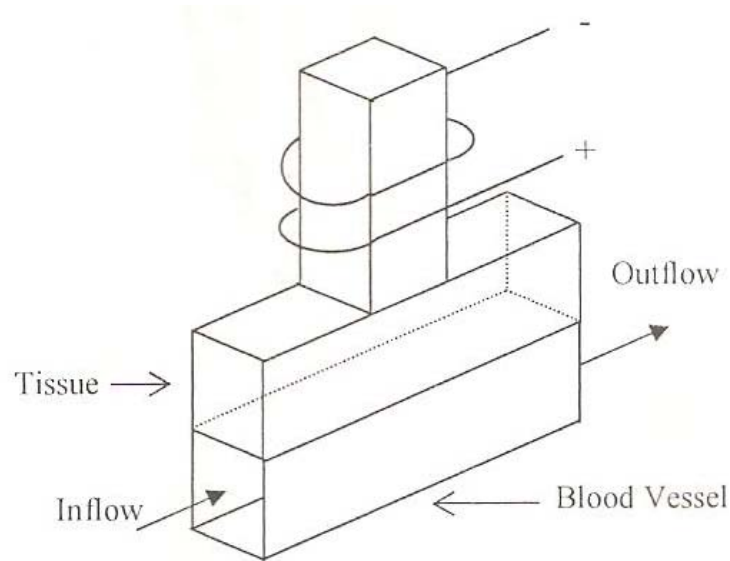


Figure 2-11: 3D geometry of blood vessel

Magnetic potential was calculated for static mode and results were used to calculate velocity field by Navier-Stokes equations in transient mode. Results for this analysis show the peak velocity of the fluid around 0.3 m/s . Figure 2-12 [27] show the velocity field obtained in the model evaluation.

Kraub, et al. [28] presented a pumping device by magnetic surface stress. The system which has a magnetic field rotating on the free surface of a ferrofluid layer induce a considerable fluid motion towards the direction the field is rolling. Experimental setup, shown in fig. 2-13 [28], is compounded of a circular duct with a mean diameter $d = 100\text{mm}$ and a square cross-section of $5\text{mm} \times 2.5\text{mm}$ and $10\text{mm} \times 10\text{mm}$. The orientation of the two coils producing the rotating magnetic field is shown in fig 2-13. In the schematic image one coil is wrapped around this

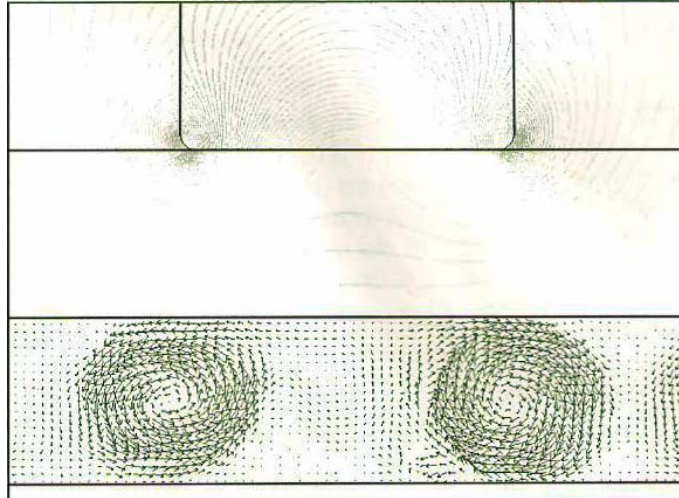


Figure 2–12: Fluid velocity field with magnetic flux density circular channel providing a magnetic field in the azimuthal direction. The outer coil produces the vertical component of the magnetic field. Coils are fed by an ac current of different phase of $90^\circ C$. Thus producing a rotating field on the free surface of the fluid within the duct.

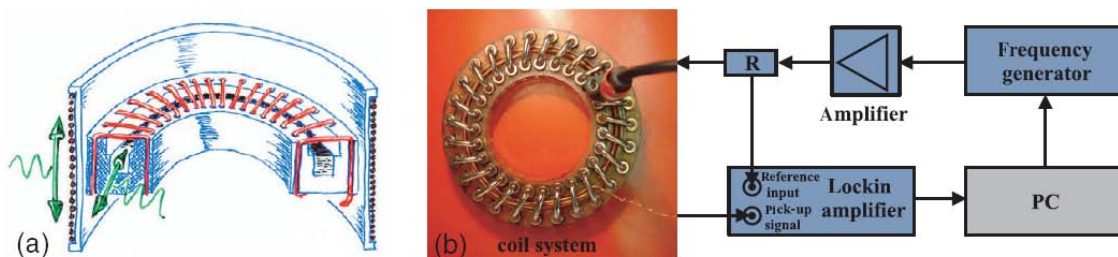


Figure 2–13: Experimental setup achieved by Kraub

Results for this experimental configuration, show that a rotating field produced by the coils leads to a motion of the fluid in azimuthal direction of the channel. The velocity achieved by the device was in the order of $mm s^{-1}$, determined by visual inspection of tracer particles swimming on its surface. It was observed that the fluid direction changed its sign when current phase was inverted from $+90$ to -90 .

Magnetite fluid sample and cobalt fluid sample are compared for 10 kHz and 1 kHz respectively in fig. 2–14(a)[28]. As indicated in fig 2–14(b) [28] higher velocity is reached by the cobalt sample.

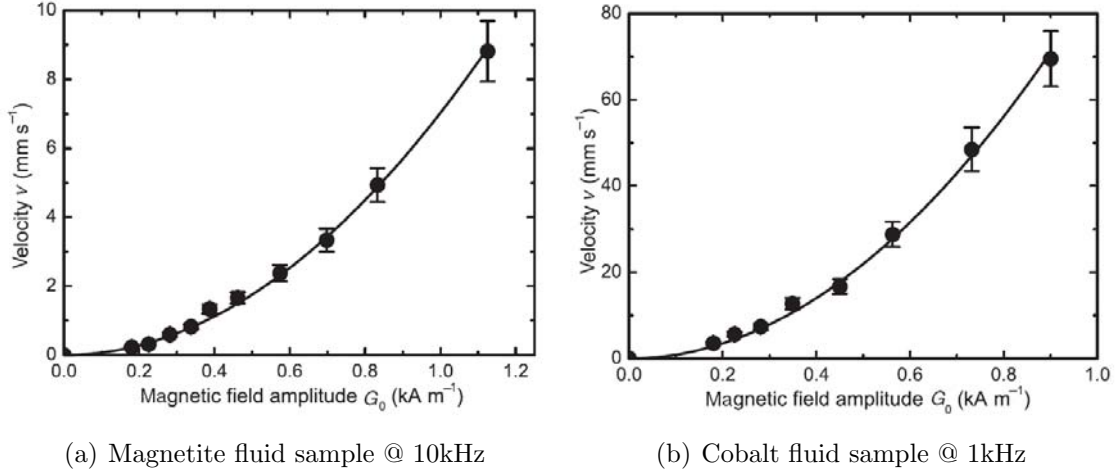


Figure 2-14: Maximal velocity measure as function of the field amplitude

2.3 Contribution of this research

Most of the contribution to pumping device using ferrofluid is related to magnetocaloric effect [29–31]. Another type of system to produce ferrofluid motion is by electromagnet oscillating mechanism. Electromagnet based pumping device is an attractive way to transport ferrofluid by a magnetic field supplied in a controllable manner.

A numerical model of both magnetic and dynamics equations for ferrofluid was developed. Simulations for magnetostatic relations were carried out into account the power sequence for the solenoids inputs. It was possible to run the simulation by adding a time function for the current density J_f . In this way the current density can be 0 or J_f depending on the turning on of the 5 solenoids in the prototype.

Taking the optimal configuration in the numerical model, the prototype was fabricated. Then, preliminary tests were performed to demonstrate the concept. Five coils, distributed around a loop of 10 mm in diameter, were constructed. A group of solenoids produce a magnetic field that are power by an electronic circuit in a sequential way in order to change the field around the pipe system.

Solenoids wrapped around the pipe concentrate the magnetic field into the fluid making stronger the field at the center because of the ferrofluid permeability μ_r . This is a novel electromagnetic pumping device using a ferrofluid.

CHAPTER 3

MATHEMATICAL FORMULATION

This formulation relates the magnetic flux density in terms of a vector potential A. The target is to obtain the magnetic force to be used in Navier Stokes equation. This force is the link between the magnetostatic and dynamics fluid phenomenon [32, 33] .

A finite element package performs the solution for ferrofluid velocity solving the magnetostatic relations, afterwards the software store this solution to use it in Navier-Stokes equation.

The mesh is a non structured type, and finite elements are used to find solution of the equations.

3.1 Magnetostatic Relations

In this section, a brief discussion of the magnetic force induced in a ferrofluid is presented. this force is the driving force for the ferrofluid motion.

The magnetic force \mathbf{f} in a charge Q moving with velocity \mathbf{v} in a magnetic field \mathbf{B} is given by:

$$\mathbf{f} = Q(\mathbf{v} \times \mathbf{B}) \quad \text{and} \quad \mathbf{v} = \mathbf{l}/t$$

$$\mathbf{f} = \frac{Q}{t}(\mathbf{l} \times \mathbf{B}) \quad \text{but} \quad \mathbf{i} = \frac{Q}{t}$$

$$\mathbf{f} = \mathbf{i}(\mathbf{l} \times \mathbf{B}) \quad (3.1)$$

For a rectangular magnetic dipole, shown in figure 3-1 from[34] and applying equation (3.1) for sides Δx and Δy

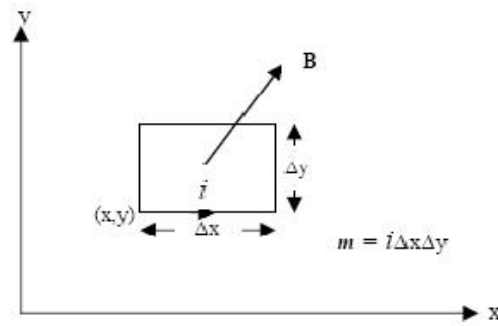


Figure 3-1: A magnetic dipole in a magnetic field \mathbf{B}

thus,

$$\mathbf{f} = \mathbf{idl} \times (B_x \mathbf{i}_x + B_y \mathbf{i}_y + B_z \mathbf{i}_z) \quad (3.2)$$

$$\mathbf{f}(x) = -\mathbf{i}\Delta y [-B_x \mathbf{i}_z + B_z \mathbf{i}_x]_x \quad (3.3)$$

$$\mathbf{f}(x + \Delta x) = \mathbf{i}\Delta y [-B_x i_z + B_z i_x]_{x+\Delta x} \quad (3.4)$$

$$\mathbf{f}(y) = \mathbf{i}\Delta x [B_y i_z - B_z i_y]_y \quad (3.5)$$

$$\mathbf{f}(y + \Delta y) = -\mathbf{i}\Delta x [B_y i_z - B_z i_y]_{y+\Delta y} \quad (3.6)$$

Summarizing all forces acting on the dipole,

$$\mathbf{f} = f(x) + f(x + \Delta x) + f(y) + f(y + \Delta y) \quad (3.7)$$

Substituting equations (3.3) to(3.6) in (3.7) yields:

$$\begin{aligned} \mathbf{f} = -\mathbf{i}\Delta x \Delta y & \left[\frac{B_z(x + \Delta x) - B_z(x)}{\Delta x} i_x - \frac{B_z(x + \Delta x) - B_x(x)}{\Delta x} i_z \right. \\ & \left. + \frac{B_z(y + \Delta y) - B_z(y)}{\Delta y} i_y - \frac{B_y(y + \Delta y) - B_y(y)}{\Delta y} i_z \right] \end{aligned} \quad (3.8)$$

The terms in the bracket define the partial derivatives in the limit of infinitesimal Δx and Δy . The coefficient is the magnetic dipole moment \mathbf{m}_z , defined in the fig. 3-1

$$\lim_{\substack{\Delta x \rightarrow 0 \\ \Delta y \rightarrow 0}} \mathbf{f} = \mathbf{m}_z \left[\frac{\partial B_z}{\partial x} i_x - \left(\frac{\partial B_x}{\partial x} + \frac{\partial B_y}{\partial y} \right) i_z + \frac{\partial B_z}{\partial y} i_y \right] \quad (3.9)$$

Expanded Ampere's and Gauss's law relate the field components for the magnetic field as follow,

$$\nabla \cdot \mathbf{B} = 0 \Rightarrow \frac{\partial B_z}{\partial z} = - \left(\frac{\partial B_x}{\partial x} + \frac{\partial B_y}{\partial y} \right) \quad (3.10)$$

$$\begin{aligned} \nabla \times \mathbf{B} = \mu_0 (\mathbf{J}_f + \nabla \times \mathbf{M}) = \mu_0 \mathbf{J}_T \Rightarrow \frac{\partial B_z}{\partial y} - \frac{\partial B_y}{\partial z} &= \mu_0 J_{Tx} \\ \frac{\partial B_x}{\partial z} - \frac{\partial B_z}{\partial x} &= \mu_0 J_{Ty} \\ \frac{\partial B_y}{\partial x} - \frac{\partial B_x}{\partial y} &= \mu_0 J_{Tx} \end{aligned} \quad (3.11)$$

which reduces equation 3.9 for the magnetic force per unit volume to the form

$$\begin{aligned} \mathbf{f} &= \mathbf{m}_z \left[\frac{\partial B_x}{\partial z} \mathbf{i}_x + \frac{\partial B_y}{\partial z} \mathbf{i}_y + \frac{\partial B_z}{\partial z} \mathbf{i}_z - \mu_0 (\mathbf{J}_{Ty} \mathbf{i}_x - \mathbf{J}_{Tx} \mathbf{i}_y) \right] \\ &= (\mathbf{m} \cdot \nabla) \mathbf{B} + \mu_0 \mathbf{m} \times \mathbf{J}_T \end{aligned} \quad (3.12)$$

Where \mathbf{J}_T is the sum of the magnetization and free current

If there are N dipole per unit of volume the Magnetic force on the free currents is,

$$\mathbf{F} = Nf = (\mathbf{M} \cdot \nabla) \mathbf{B} + \mu_0 \mathbf{M} \times \mathbf{J}_T + \mathbf{J}_f \times \mathbf{B} \quad (3.13)$$

Using the constitutive equation for the magnetic field $\mathbf{B} = \mu_0(\mathbf{H} + \mathbf{M})$ and

$$\mathbf{J}_T = \mathbf{J}_f + \nabla \times \mathbf{M}$$

$$\begin{aligned} \mathbf{F} &= \mu_0 (\mathbf{M} \cdot \nabla) (\mathbf{H} + \mathbf{M}) + \mu_0 \mathbf{M} \times (\mathbf{J}_f + \nabla \times \mathbf{M}) + \mu_0 \mathbf{J}_f \times (\mathbf{H} + \mathbf{M}) \\ &= \mu_0 (\mathbf{M} \cdot \nabla) (\mathbf{H} + \mathbf{M}) + \mu_0 \mathbf{M} \times (\nabla \times \mathbf{M}) + \mu_0 \mathbf{J}_f \times \mathbf{H} \end{aligned} \quad (3.14)$$

Using vector identity

$$\mathbf{M} \times (\nabla \times \mathbf{M}) = -(\mathbf{M} \cdot \nabla) \mathbf{M} + \frac{1}{2} \nabla (\mathbf{M} \cdot \mathbf{M}) \quad (3.15)$$

Equation (3.15) is substituted in (3.14) in order to obtain,

$$\mathbf{F} = \mu_0 (\mathbf{M} \cdot \nabla) \mathbf{H} + \mu_0 \mathbf{J}_f \times \mathbf{H} + \nabla \left(\frac{\mu_0}{2} \mathbf{M}^2 \right) \quad (3.16)$$

In this analysis, an arbitrary control volume is considered which is fully submerged within the ferrofluid. Thus, the last term in eq.(3.16) is not necessarily zero. For non conductive fluid $\mathbf{J}_f = 0$. Under these considerations equation (3.16) becomes:

$$\mathbf{F} = \mu_0 (\mathbf{M} \cdot \nabla) \mathbf{H} + \nabla \left(\frac{\mu_0}{2} \mathbf{M}^2 \right) \quad (3.17)$$

This is the magnetic force acting on the ferrofluid.

Expanding equation 3.17 in cylindrical coordinates gives:

$$\begin{bmatrix} F_r \\ F_\phi \\ F_z \end{bmatrix} = \mu_0 \begin{bmatrix} M_r \frac{\partial H_r}{\partial r} + M_\phi \frac{1}{r} \frac{\partial H_r}{\partial \phi} + M_z \frac{\partial H_r}{\partial z} \\ M_r \frac{\partial H_\phi}{\partial r} + M_\phi \frac{1}{r} \frac{\partial H_\phi}{\partial \phi} + M_z \frac{\partial H_\phi}{\partial z} \\ M_r \frac{\partial H_z}{\partial r} + M_\phi \frac{1}{r} \frac{\partial H_z}{\partial \phi} + M_z \frac{\partial H_z}{\partial z} \end{bmatrix} + \frac{\mu_0}{2} \begin{bmatrix} \frac{\partial M^2}{\partial r} \\ \frac{1}{r} \frac{\partial M^2}{\partial \phi} \\ \frac{\partial M^2}{\partial z} \end{bmatrix} \quad (3.18)$$

Cylindrical coordinates are chosen to take advantage of the cylindrical symmetry at the pipe. So, one of the components (F_ϕ) is zero by symmetry. The remaining quantities are independent of ϕ . Now the magnetic force can be reduced to the following equations,

$$\begin{pmatrix} F_r \\ F_z \end{pmatrix} = \mu_0 \left[\begin{pmatrix} M_r \frac{\partial H_r}{\partial r} + M_z \frac{\partial H_r}{\partial z} \\ M_r \frac{\partial H_z}{\partial r} + M_z \frac{\partial H_z}{\partial z} \end{pmatrix} + \frac{1}{2} \begin{pmatrix} \frac{\partial M^2}{\partial r} \\ \frac{\partial M^2}{\partial z} \end{pmatrix} \right] \quad (3.19)$$

The force \mathbf{F} depends on \mathbf{H} and \mathbf{M} . These fields are obtained from the solution of the Maxwell equations and constitutive equation of the ferrofluid.

$$\nabla \cdot \mathbf{B} = 0 \quad \text{Gauss law for magnetism} \quad (3.20)$$

$$\mathbf{B} = \nabla \times \mathbf{A} \quad \text{Curl of vector field} \quad (3.21)$$

$$\mathbf{B} = \mu_0 (\mathbf{H} + \mathbf{M}) \quad \text{Constitutive equation} \quad (3.22)$$

$$\nabla \times \mathbf{B} = \mu_0 \mathbf{J}_f \quad \text{Ampere law} \quad (3.23)$$

Where,

\mathbf{B} is the magnetic field intensity in Tesla,

\mathbf{H} is the magnetic field in A/m

\mathbf{M} is the magnetism of the ferrofluid in A/m

\mathbf{A} is the vector potential

\mathbf{J}_f is the source density current in A/m²

μ_0 is the magnetic permeability of free space with value of $4\pi \times 10^{-7} \text{N/A}^2$

The magnetic field intensity \mathbf{B} will be obtained by solving for vector field \mathbf{A} ,

Taking the curl of \mathbf{B} in equation (3.21) and substituting into equation (3.23)

$$\nabla \times \nabla \times \mathbf{A} = \mu_0 \mathbf{J}_f \quad (3.24)$$

From vector identity $\nabla \times \nabla \times \mathbf{A} = \nabla (\nabla \cdot \mathbf{A}) - \nabla^2 \mathbf{A}$

now, taking an arbitrary value for $\nabla \cdot \mathbf{A}, \nabla \cdot \mathbf{A} = 0$ This is the Coulomb gauge

which is selected for convenience,

$$\nabla^2 \mathbf{A} = \mu_0 \mathbf{J}_f \quad (3.25)$$

Substituting vector field \mathbf{A} in (3.21), which is solved from Poisson equation in (3.25)

knowing the source density current \mathbf{J}_f , \mathbf{B} is obtained. Substituting \mathbf{B} in equation (3.22) \mathbf{H} is obtained. Finally, by substituting \mathbf{H} and \mathbf{M} in (3.19), the solution of the magnetic force \mathbf{F} is obtained.

\mathbf{J}_f is the *current density*, necessary to solve the vector potential \mathbf{A} in (3.25). The value of \mathbf{J}_f is limited by the wire diameter. In the model developed, different values of \mathbf{J}_f were evaluated in order to determine the optimal wire diameter to be used in the prototype.

$$\mathbf{J}_f = I/S_c \quad (3.26)$$

Where, I is the current in Ampere passing the conductor; S_c is the cross sectional area of the conductor. These calculations are detailed in the solenoid design, presented in the appendix [A](#)

\mathbf{H} is the *magnetic field* generated by the electromagnets and function of J_f .

M is the *ferrofluid magnetization*, which is a function of the magnetic field H which is obtained experimentally from M vs H curve. Fig. 3–2 is a typical M - H curve. Values of M are obtained by interpolation from different H . A function of M is supplied to the simulation software. The data for this function was experimentally obtained for different magnetic field applied and different temperatures [35].

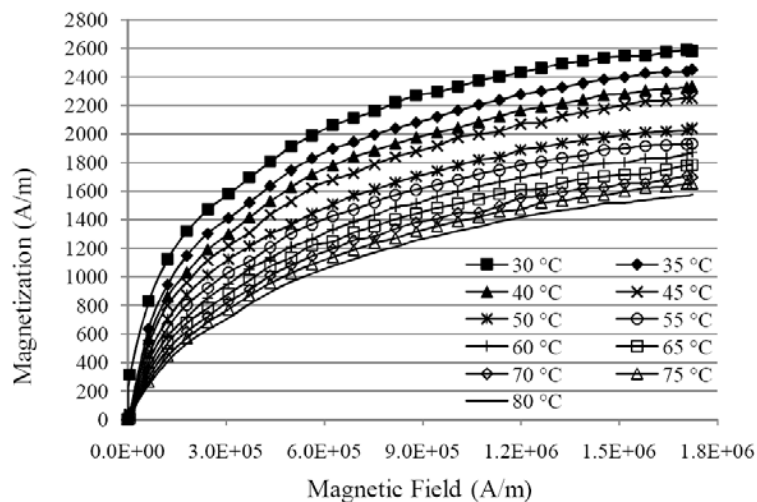


Figure 3–2: Magnetization-Magnetic field curve for different temperature

3.2 Ferrofluid flow formulation

The magnetic force is the driving force for the ferrofluid flow exposed to an external magnetic field. Navier-Stokes equation are solved in order to obtain the velocity profile in the ferrofluid. These equations are the continuity and momentum equations. The fluid equation are stated as fallows:

$$\frac{\partial \rho}{\partial t} + \rho \nabla \cdot \mathbf{v} = 0 \quad (3.27)$$

$$\rho \left(\frac{\partial \mathbf{v}}{\partial t} + (\mathbf{v} \cdot \nabla) \mathbf{v} \right) = -\nabla P + \eta \nabla^2 \mathbf{v} + \mu_0 (\mathbf{M} \cdot \nabla) \mathbf{H} \quad (3.28)$$

where,

$P = P_T - P_s - P_{mag} = P_T - \rho(\mathbf{g} \cdot \mathbf{r}) - \frac{\mu_0}{2} \mathbf{M}^2$ is the dynamic pressure.

$\rho \frac{\partial \mathbf{v}}{\partial t}$ is the rate of change of momentum; net acceleration.

$\rho(\mathbf{v} \cdot \nabla) \mathbf{v}$ is the convective acceleration.

∇P is the pressure force.

$\eta \nabla^2 \mathbf{v}$ is the viscous force.

$\mu_0 (\mathbf{M} \cdot \nabla) \mathbf{H}$ is the Kelvin force.

As discussed before, symmetry was taken into consideration for axis symmetric flow. The tangential velocity is canceled, ($u_\varphi = 0$), and the derivatives respect to φ also cancel. Then, the continuity equation is:

$$\frac{1}{r} \frac{\partial}{\partial r} (ru_r) + \frac{\partial u_z}{\partial z} = 0 \quad (3.29)$$

Momentum equation for axis symmetric coordinates

$$\rho \left(\frac{\partial u_r}{\partial t} + u_r \frac{\partial u_r}{\partial r} + u_z \frac{\partial u_r}{\partial z} \right) = -\frac{\partial p}{\partial r} + \mu \left[\frac{1}{r} \frac{\partial}{\partial r} \left(r \frac{\partial u_r}{\partial r} \right) + \frac{\partial^2 u_r}{\partial z^2} - \frac{u_r}{r^2} \right] + F_r \quad (3.30)$$

$$\rho \left(\frac{\partial u_z}{\partial t} + u_r \frac{\partial u_z}{\partial r} + u_z \frac{\partial u_z}{\partial z} \right) = -\frac{\partial p}{\partial z} + \mu \left[\frac{1}{r} \frac{\partial}{\partial r} \left(r \frac{\partial u_z}{\partial r} \right) + \frac{\partial^2 u_z}{\partial z^2} \right] + F_z \quad (3.31)$$

Where, F_r and F_z are the components of the magnetic force acting on the ferrofluid.

3.3 Solver package

The application used for numerical simulations was a finite-element mesher and solver called COMSOL Multiphysics v3.5. The model developed was simulated in two applications. In the first application, a magnetic system is developed for magnetic force calculation. In the second application a dynamic fluid system was solved for the flow velocity.

Detail parameters for the model alaboration are presented in the following table

Number of domain of the model	7
Nuber of Boundaries	35
mesh type	Triangular, non structured
Number of mesh points	131,853
Linear System solver	Direct (UMFPACK)
Analysis type	Transient

3.4 Proposed numerical model

The model proposed is a multiphysics problem including a magnetostatic and Navier-Stokes modules, see fig. 3–3. domains were selected as follows:

- Axial symmetry pipe, which will be the medium for fluid flow.

- Magnets, this is equivalent to axial symmetric cross sectional of the solenoids.
- A big domain is set up in order to vanish the magnetic field far from the center.

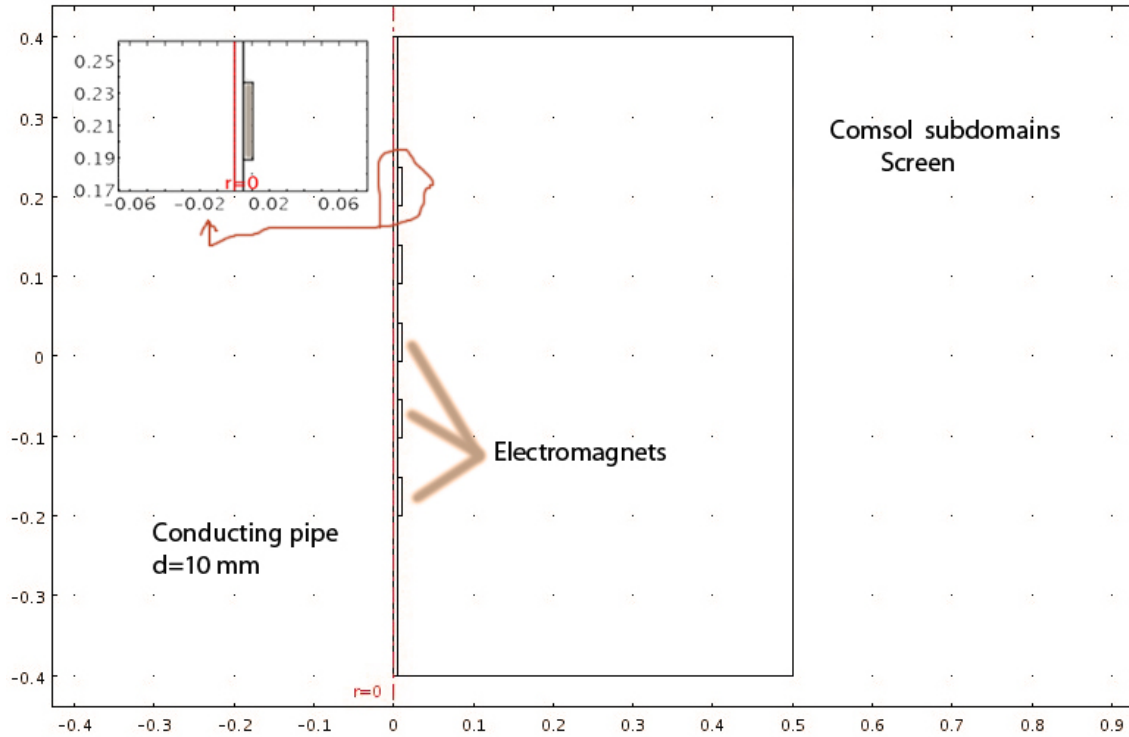


Figure 3-3: Model view in the COMSOL window

3.5 Boundaries conditions

Ferrofluid flow motion can be analyzed by integrating two modules. These modules are magnetostatic and fluid dynamic module. Coupling between both phenomenon is the Kelvin Force, discussed before. In order to solve the systems of equations, it is necessary to select suitable boundary conditions. Different types of boundary conditions are used for magnetostatic and fluid dynamic equations. Details of these boundaries conditions are presented in the following section for the particular model described earlier.

3.5.1 Boundaries conditions for the magnetostatic field

- Magnetic potential $A = 0$ define the magnetic isolation in the boundaries. Due to axial symmetric axis selected, magnetic field is equal to zero in the normal component.
- The continuity boundary condition $n \times (\mathbf{H}_1 - \mathbf{H}_2) = 0$ is the natural boundary condition implying continuity of the tangential component of the magnetic field.

3.5.2 Boundary conditions for Navier Stokes equations

- $u = 0$ Non slip velocity at the walls of the pipe. The no slip boundary condition is applicable for stationary solid walls.
- $\frac{\partial u}{\partial r} = 0$ The axis symmetry boundary condition prescribes and vanishing stresses in the z direction. It is used on all boundaries with coordinate $r = 0$.
- The periodic boundary condition is used to define two quantities equal on two different boundaries. In this case, the periodicity is applied to the velocity field and pressure.

CHAPTER 4

METHODOLOGY

The research objectives, described in chapter 1 have been divided in 4 sections which are: the operation, working fluid, coil design and design parameters.

1) Operations: this section treats about the prototype performance and operation parameters. 2) The working fluid: is a ferrofluid suspension in water carrier fluid with magnetic properties. 3) Coil design: design of five solenoids taking into account the magnetization generated by a power coils [36]. And 4) Design parameters of the device: Components and pieces of equipments (acesories) required to elaborate the characterization of the prototype.

4.1 Operation

A magnetic field generated by a solenoid will be capable to exert a magnetic body force on a ferrofluid. Five solenoids along 0.15 meter loop are wrapped around 11 mm diameter pipe as is shown in figure 4-1.

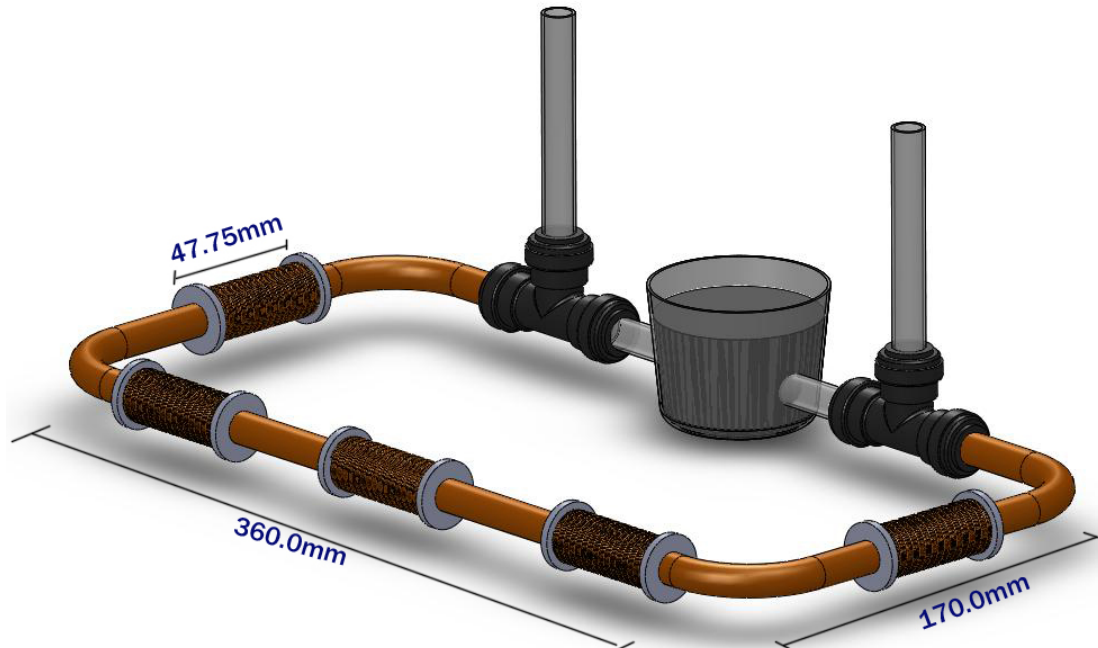


Figure 4-1: Electromagnet pump device

In order to supply a moving force to ferrofluid, the coils are rolled on the loop at the same distance. Power is supplied to the solenoid by a 24V DC source, an electronic circuit achieves the sequence necessary to produce a moving magnetic field. Only one solenoid is powered on in a fraction of time. The next solenoid is powered on after a time step has elapsed and while others solenoids stay in power off mode see fig. 4-2. Due to the moving magnetic field, the ferrofluid inside the is be affected by this field and a fluid flow is established as the solenoids power on and the sequence is initialized.

A 24V DC electronic circuit is set to provide the power supply to the solenoids. In order to obtain a moving magnetic field, a control unit capable to provide a step

output voltage cyclically to the solenoids is required. The main components of the control unit are presented in fig. B-4 and fig. B-5

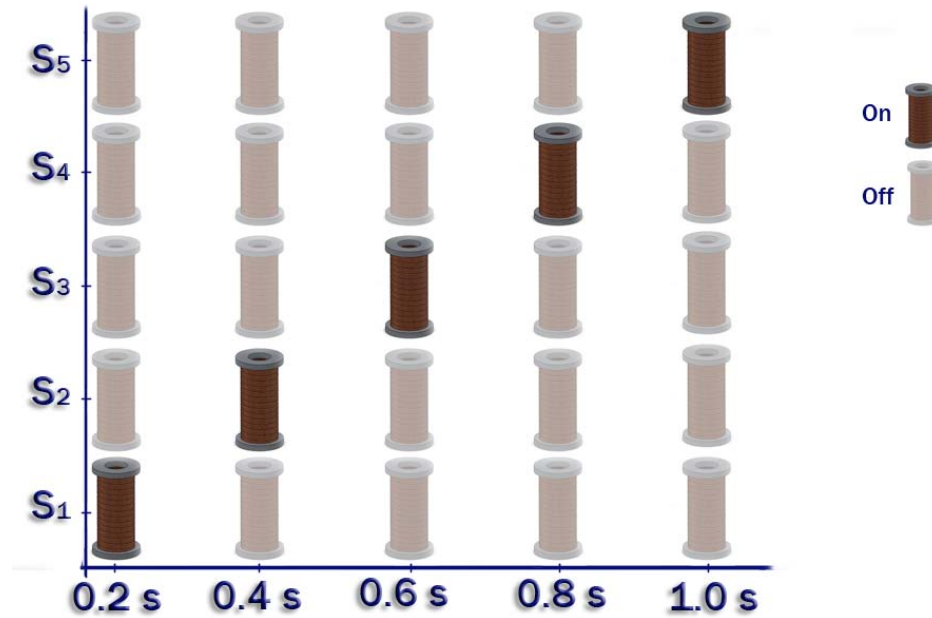


Figure 4-2: Time sequence for the operation of the solenoids

4.2 Working fluid

Fluid flowing through the electromagnet pump configuration is water based Mn-Zn ferrofluid ($Mn_{0.5}Zn_{0.5}Fe_2O_4$). Characterization of the magnetic behavior of the ferrofluid and the nanoparticles powder was achieved using a VSM magnetometer [35]. Dynamic viscosity and density for this ferrofluid are $\mu = 0.5279 \times 10^{-3} Pa.s$ and $\rho = 1087.23 kg/m^3$ respectively [35]. The particle size was aprox. 10nm according to HRTEM in [21]. The volume fraction for the ferrofluid was found to be $\phi = 4.84\%$ and it was calculated doing the quotient between the saturation magnetization of the ferrofluid and the saturation magnetization of the ferrite, both at the same temperature [20]. Due to the developed device operative temperature can be the room temperature, the pyromagnetic coefficient and demagnetization temperature are not relevant issue. For this reason, the main property requirement for ferrofluids is a high susceptibility at room temperature.

4.3 Coil design

The coil constructed is wrapped in a copper ferrofluid loop. According to the dimension of the loop, 5 solenoids are distributed along the loop as shown in fig. 4-3

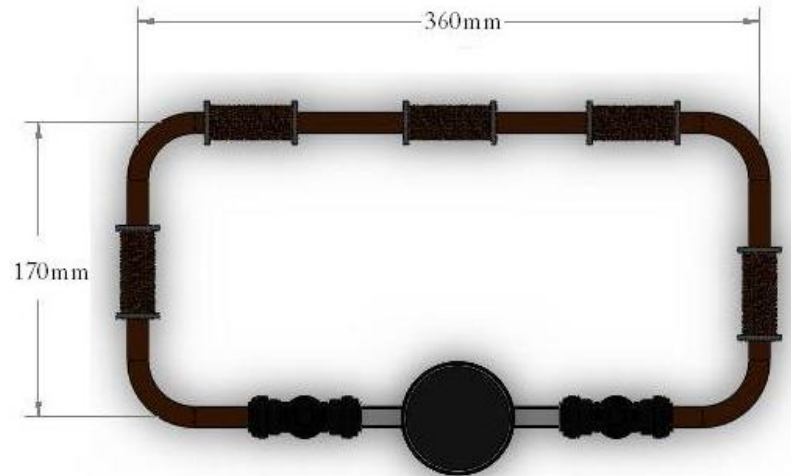


Figure 4-3: Distribution of coils along the ferrofluid loop

The first data needed in order to build the coil is the axial length. With this measure it is possible to calculate the number of the turn which will be detailed next. Fig. 4-4 is a sectional view of a coil. The core of solenoid has a diameter equal to the exterior diameter of the pipe. That is, the core will be the ferrofluid passing by the pipe.

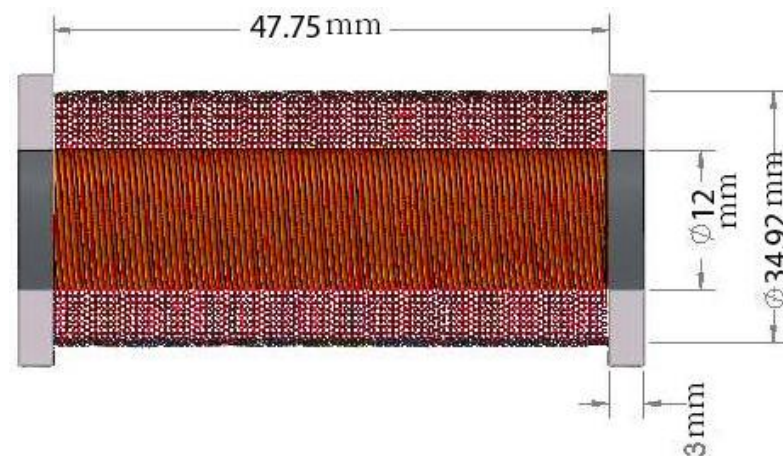


Figure 4-4: Cross section view of a solenoid to be wrapped on the loop

Table 4–1: a) Coil data, see figure 4–4; b) Wire data are (These parameters were used to build the solenoids)

a)			b)		
Core Radius (mm)	r_1	6.00	Wire size	(AWG)	24
Core Diameter (mm)	D_1	12.00	Diameter (mm)	D	0.511
Outer Radius (mm)	r_2	17.46	Nom Diameter (mm)	d_c	0.540
Coil Diameter (mm)	D_2	34.93	Turns/length	T/cm	19.60
Coil Thickness (mm)	R_A	11.46	Turn/Area	T/mm^2	2.77
Core Length (mm)	l_m	47.75	Resistivity	ohms/km	84.22

Using parameters from table 4–1, the number of turns of the coil can be calculated using following equations,

$$N_{layers} = \frac{R_A}{d_c} \quad (4.1)$$

Being l_m the axial length of the coil, the number of turn per layer of the coil will be

$$N_{turn/layers} = \frac{l_m}{d_c} \quad (4.2)$$

knowing the values in equations (4.1) and (4.2) it is easy to determine the total number of turns of the coil by following relation,

$$N = N_{layers} N_{turn/layers} \quad (4.3)$$

The results give the specifications of the solenoids required in the prototype proposed,

Table 4–2: Summary of the solenoids design parameters

Total Number of turns (turns)	1514.5
Total Resistance (Ohms)	8.90
Applied V (DC voltage)	24
Rated current (Amp)	2.70
Current Density (A/M^2)	1.29×10^7

4.4 Control unit

This section is presented in the Appendix B, p. 58

4.5 Design parameters of the device

In order to investigate the behavior of ferrofluids influenced by a magnetic field, simulations for different situations have been achieved. Afterwards, the development of a prototype have been built to perform the analysis achieved in simulations. Components used in the prototype are listed in the table 4-3

Table 4-3: Materials to develop the electromagnet pumping device

Item	Description	Quantity	Application
1	Wire pack awg 24	2	Coil construction
2	Epoxy tube	1	Hold the coils to pipe
3	Breadboard	1	Tasting the circuit
4	Transistors TIP31B	10	Commutator
5	Microcontroller 16f84	1	Sequence power to coils
6	3 position switch	1	Variation of the time step
7	Coated wire	3ft	For connections
8	Multimeter	1	Monitoring parameters
9	Power supply 24v DC	1	For coils power supply
10	Screws,	2	Minors activities
11	Ferrofluid	100 ml	Working fluid
12	Copper 12mm ϕ	0.5m	Pipe of the system
13	T pvc connectors	2	To fill up the system
14	Aluminum bar	10in	Disc for hold the coils
15	Gaussmeter	1	Magnetic field measurements
16	Led diode	10	Indications
17	Adhesive Tape	1	To cover the coils and wires
18	Resistances	20	For current limitation
19	Capacitors	2	For oscillation current protection
20	Power supply 5v DC	1	For control circuit power feed

CHAPTER 5

RESULTS

In this section the results of the research is presented and discussed. The discussion includes: solenoid design, numerical simulations of the device and finally, preliminary results of the prototype developed.

5.1 Results of the design of the solenoid

Coil axial length

The ferrofluid pump device driven by electromagnets comprises a 12mm ϕ and 0.5m length loop surrounded by solenoids. The axial length of the coil is related to the core diameter of the coil. The optimal length of the coil is equal to 4 times the diameter of the core of this. Five solenoids were distributed equidistant around the loop.

Wire size

A tolerance of 20% of the maximum current delivered by the power supply was taken to avoid damage to the source. Then, the average current that would flow through the coil would be 4A with a voltage of 24V DC. Based on the current rating, the diameter of the wire used for the coil was selected. According to the American Wire Gauge (AWG) standard [37] , the size of wire to carry 4A must be AWG 20

or less. By using a smaller diameter wire would produce heating due to the IR^2 effect. This, would degrade the wire coating used as insulation and damage the coil. Nevertheless, as the solenoid will operate in pulsed mode, the current can be increased or the wire size can be reduced. For this reason a size of the wire was selected as AWG 24 to fabricate the solenoids.

Coil thickness

As the coil is wrapped on the pipe, the core of the coil would be equal to the outer diameter of the pipe. the radial distance or thickness of the coil would be given by the difference between the radius of the coil and the core radius of the coil. See fig.1-2 and 4-4. The thickness for the coil was **11.46mm**.

Number of turns

From data of wire size, the coil axial length and radial distance, the number of turns was calculated using the equation 4.1 to 4.3. The value obtained for the number of turns for each coil was **1514 turns**.

Current density

Using the dimensions of the designed coil, the current density of the transverse area of the coil is the product of the conductor current density (A.24 and the number of turns of the coil. The calculated value of the current density ($J_f = 1.29 \times 10^7 A/m^2$) was obtained from the design parameters of the solenoid

5.2 Results of the numerical simulation

The calculated value of the current density is an input value to solve the equations of magnetostatics. The value of the current density was entered by a function of time (J_e) from coil 1 to 5. This function is used to generate the sequence of power in the numerical model.

$$J_{e1} = J_f(t > 0 \rightarrow t \leq 0.20)$$

$$J_{e2} = J_f(t > 0.20 \rightarrow t \leq 0.40)$$

$$J_{e3} = J_f(t > 0.40 \rightarrow t \leq 0.60)$$

$$J_{e4} = J_f(t > 0.60 \rightarrow t \leq 0.80)$$

$$J_{e5} = J_f(t > 0.80 \rightarrow t \leq 1.0)$$

The calculated magnetic field is the same for each coil, but generated at different times according to the time function. Fig. 5–1 show the model and Fig. 5–2 show the magnetic field generated by J_e for different times and for all solenoids.

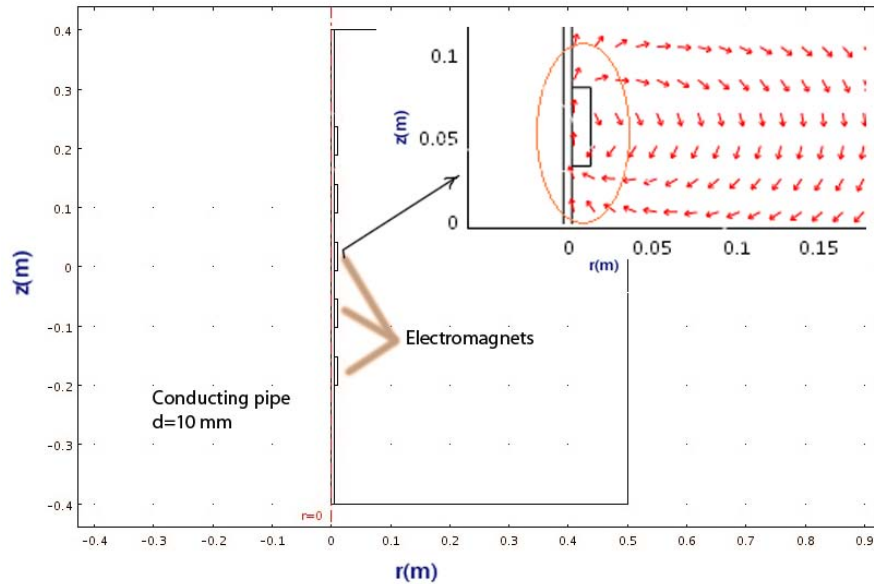


Figure 5–1: Numerical model and magnetic field in a coil

Simulations were performed for different times of operation of the coil. With this, it was observed that for very long operating periods the fluid does not react

under the applied fields. Then, as time was being reduced, the fluid started to move until it reaches the maximum flow velocity for a step time of 0.2s. When the step time was less than 0.2s the fluid slows down and eventually stopped moving.

The explanation for this effect is that, for very long periods the magnetic force generated drives the fluid toward the center of the coil from both ends of the coil. Then the resultant force in the center of the coil is zero so it does not generate motion in the fluid. For short times step the fluid moves driven by the magnetic force that moves as the field moves. And for very short periods the fluid does not respond to the field because the time is not enough for this scope magnetization. Fig 5-3 shows the magnetic field generated in different solenoids of the system.

In order to evaluate the behavior of the solenoids when higher voltage is applied. Table 5-1 shows a comparison between three different voltage. It can be seen that the greater the current density in the solenoid the higher the resultant magnetic field generated, nevertheless, to increase the voltage it is necessary to redesign the coil. This will increase the wire diameter, and the number of turns. Exceed the power limit of a solenoid will damage the insulation and therefore the coil. To avoid risk of damage to the coil, a good design must be performed before the fabrication of the prototype.

Table 5-1: Current density for different voltage applied in the model designed

Source voltage (V)	Wire current density $J_f(A/m^2)$	Model current density $J_e (A/m^2)$	Rated current I(A)
24	8.50×10^3	1.29×10^7	4.1
48	1.70×10^4	2.58×10^7	5.40
110	3.90×10^4	5.90×10^7	12.37

Flow velocity for three different voltage, is shown in fig. 5-4

Fig. 5-4 shows the behavior of the ferrofluid flow for different applied voltages. As it is seen, the higher velocity is reached for the higher applied voltage. But, as

that voltage is over the design limit in the wire, a bigger solenoid must be constructed to carry out the current density required to generate that flow velocity.

5.3 Results of the characterization

The fabrication of the prototype was carried out with a power supply capacity of 24V DC @ 5A. Power to the five solenoids was supplied in a sequential turning on order. A control circuit was designed and fabricated to produce the power sequence. Figure 5-7 and 5-6 show the electromagnet pump prototype and its circuit control.

The magnetic field was generated successfully in each solenoid. The sequence power was achieved for different time steps, from 3 second to 0.2 second per step. Preliminary results for the prototype developed show a flow motion for the shorter time step selected, which was 0.2 seconds. That means that one coil operated for 0.2 second while others four stayed power off, after that time that coil went off and the next one in the sequence went power on. This order was repeated with all the coils and checked the sequence generated by the electronic circuit.

As the magnetic body force is pretty much constant inside the pipe, the flow velocity profile is a parabolic profile. Flow velocity calculation revealed a dependence of time for velocity. Nevertheless, when as the time step is reduced the magnetic field circulates faster around the loop and velocity is higher and constant.

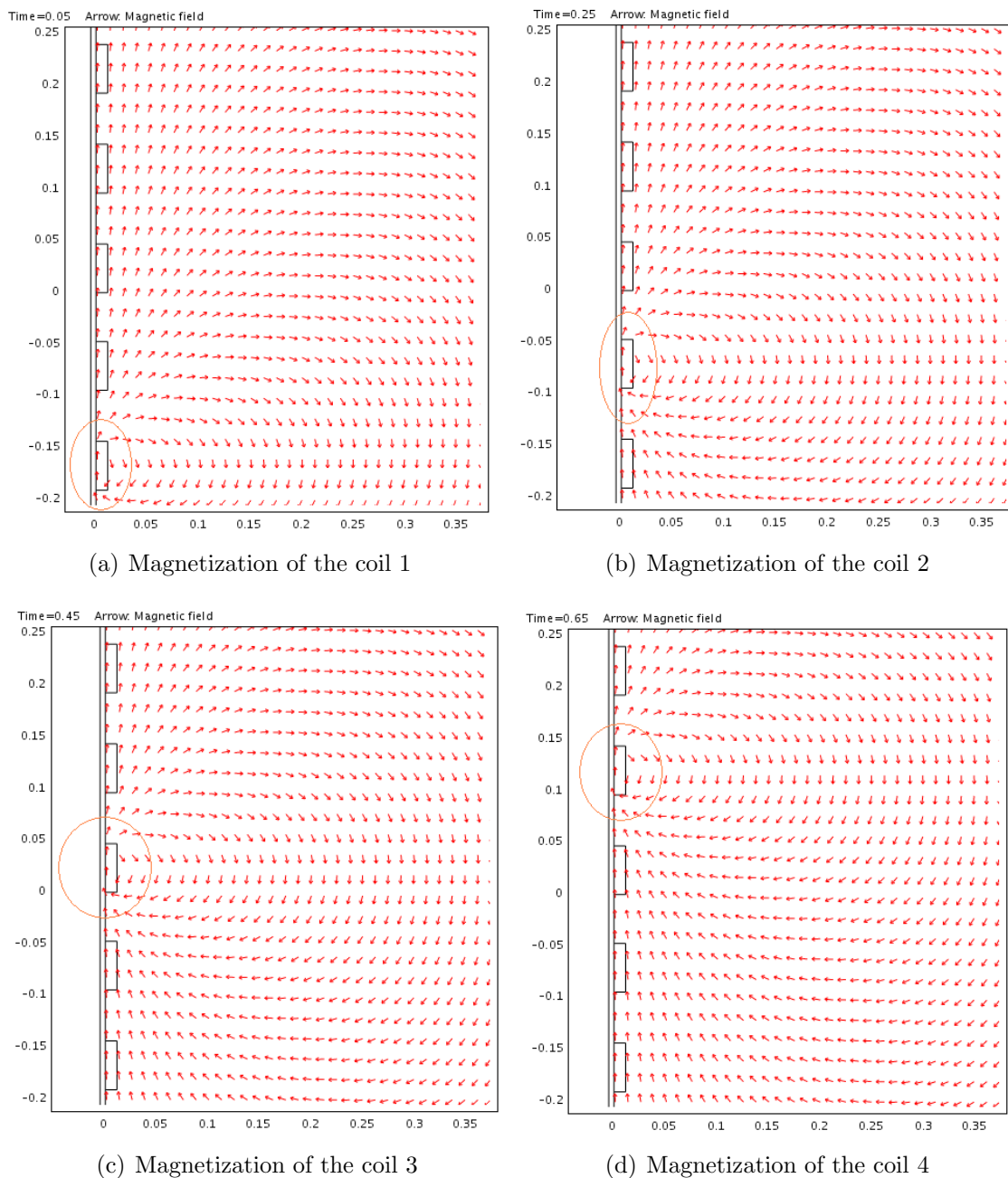


Figure 5-2: Magnetic field generated by the time function in the solenoids

Flow velocity profile for 24V solenoid input voltage

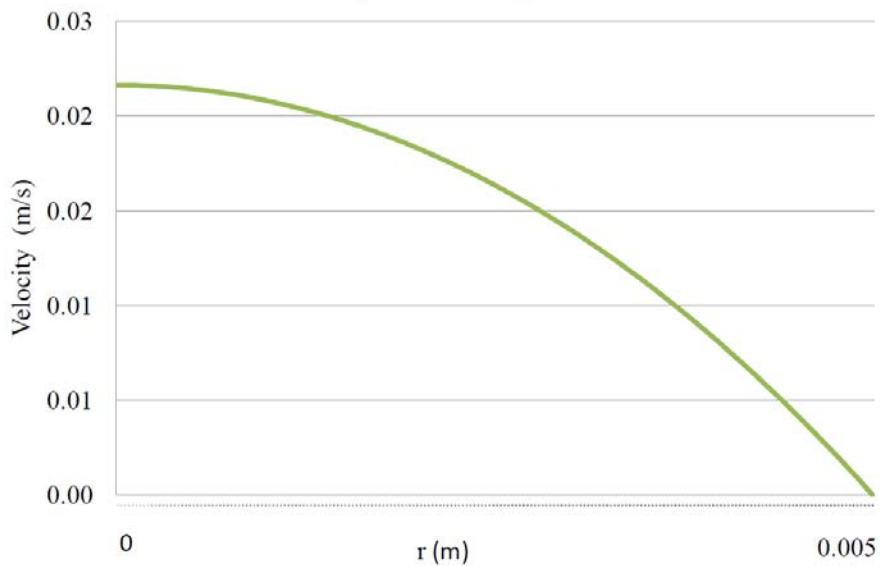


Figure 5-3: Velocity profile for the model

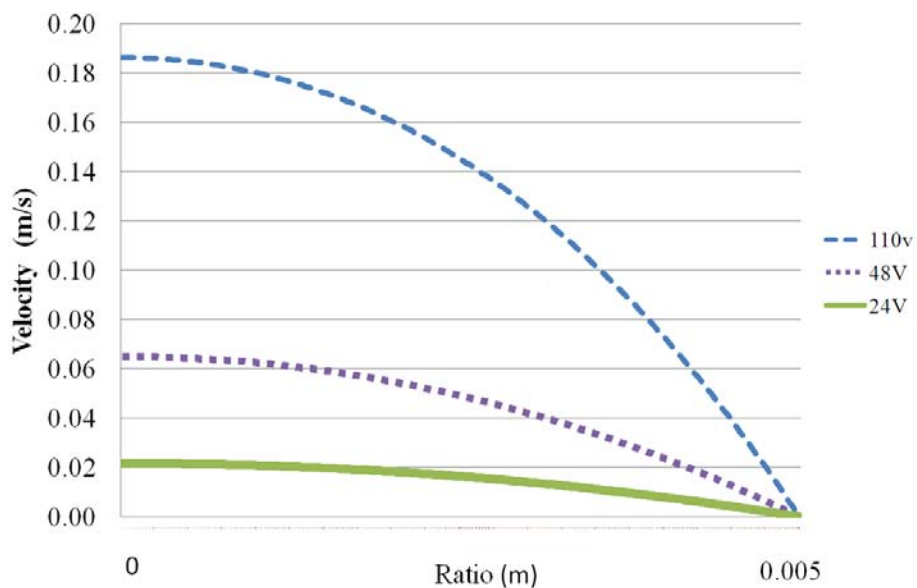


Figure 5-4: Flow velocity for 24V, 48V and 110V solenoids input voltage

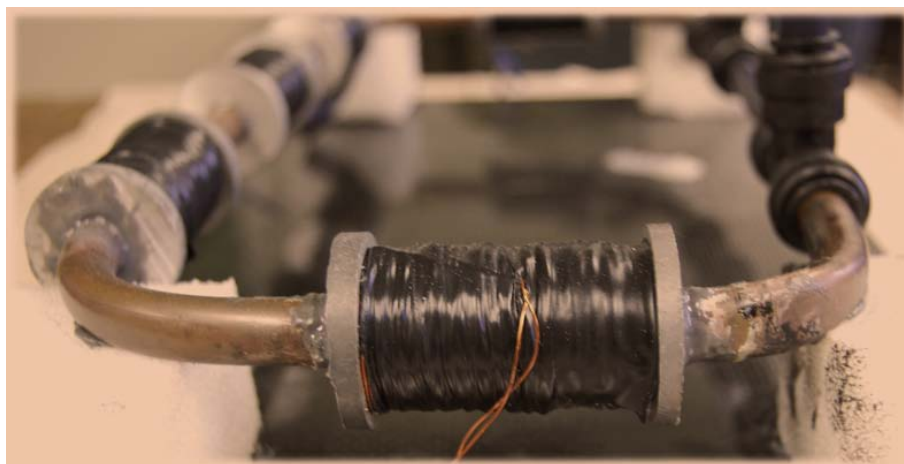


Figure 5-5: Solenoid view

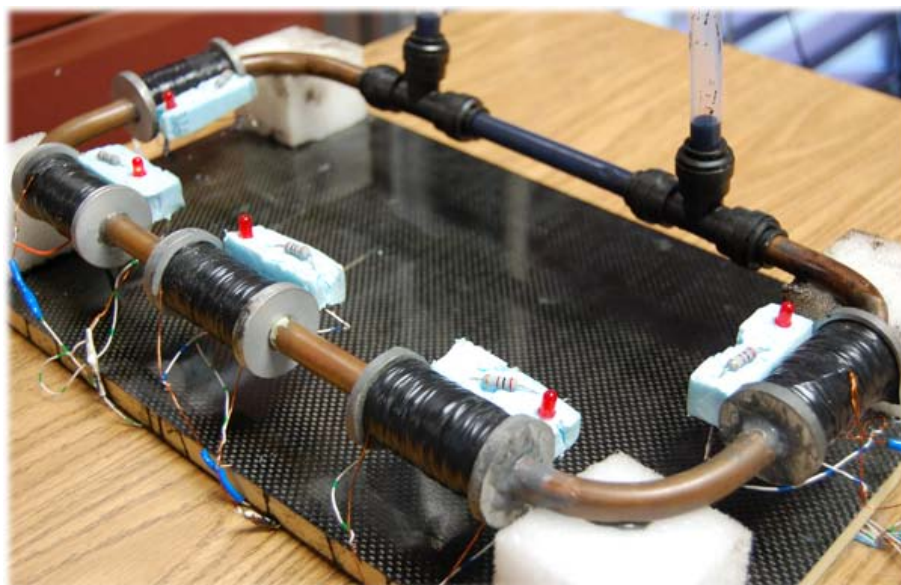


Figure 5-6: Solenoids wrapped around the loop

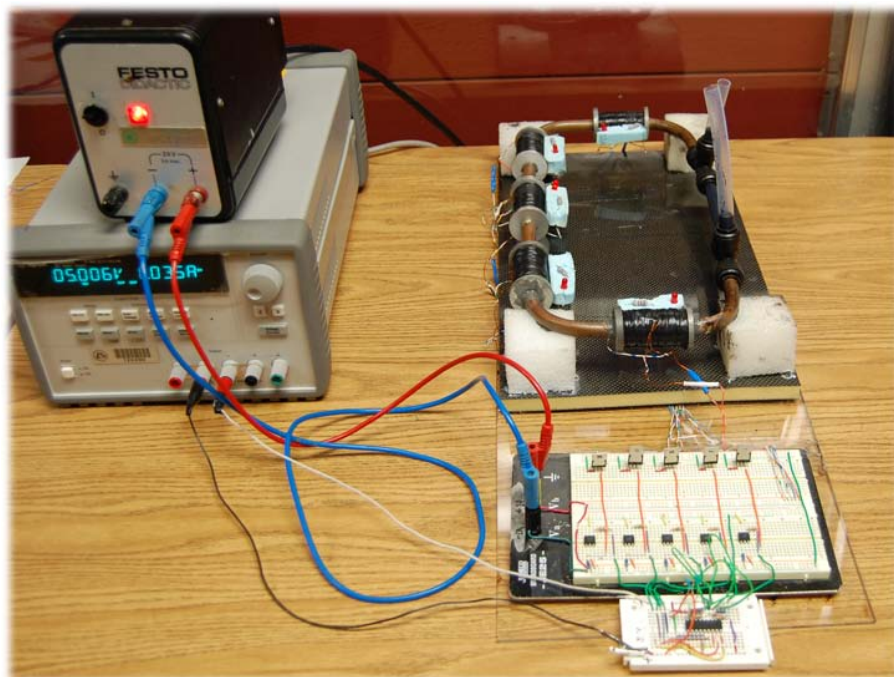


Figure 5-7: Electromagnets ferrofluid pump prototype

CHAPTER 6

CONCLUSIONS AND RECOMMENDATIONS

Conclusions

A ferrofluid pumping device, driving by electromagnets, was developed. Initially, electromagnet or solenoid was designed to evaluate operation parameters such as: the optimal size of the solenoid, rated current and power requirement. The current density J_f was obtained from various solenoids size and different source voltage.

The numerical model was performed in a finite element solver package called COMSOL Multiphysics. numerical simulations were carried out based on the optimal solenoid size and for three different current density. This three current density were related to three different voltage applied to the solenoids. The average fluid velocity in the simulations was about 22 mm/s

The prototype development was fabricated taking the appropriated model and with a feasible power source. A group of five solenoids were wrapped around a 10mm diameter loop with MnZn ferrofluid in it. Power on of these solenoids was sequenced to generate a moving magnetic field. The sequence in the solenoids operation was carried out by an electronic circuit designed for that application.

The parameters of the loop, the coil and ferrofluid were the same for the design, simulation and the prototype. This is, parameters obtained from the design were used to construct the numerical model. With the model dimensions it was constructed the prototype.

Preliminary test were done to demonstrate the concept proposed. Experimental runnings of the ferrofluid pumping device revealed some fixable issues as power

supply capacity, quantity of solenoids, type of ferrofluid and power control of the solenoids. These issues must be analyzed in order to optimize the device in future work.

Recommendations and future work

The developed prototype can be optimized to increase the flow rate. During the simulations and the characterization of the prototype some issues were found. These issues are presented below, followed by the recommendations suggested:

- *Current density*, from the analysis of the numerical simulations, the velocity of the ferrofluid increases as current density increases. This parameter is related to the size of the solenoids. By increasing the power of the solenoid a higher power source should be used. Since current is related to the magnetic field, it is obvious that a higher current will increase the magnetic field. This principle is limited by the heat generated by IR^2 relation. However, since the time that the power is on in each solenoid is pulsating, this won't be of much concern.
- *Control unit*, the electronic circuit which achieves the power control of the solenoids could be improved to enhance the pumping flow rate. With the actual circuit, the time step used to power each solenoid must be done in power off mode. By changing the time step in power on mode can be tuned with the ferrofluid frequency. This will increase the velocity due to the inertia exerted by the ferrofluid. This will increase the flow rate of the ferrofluid.
- *Solenoid configuration*, Quantity and separation of the coils can be studied. By increasing the number of the solenoids, the magnetic field can be increased in the ferrofluid. According to simulations by increasing the number of solenoids a higher flow rate was obtained.

APPENDIX A

INTRODUCTION TO ELECTROMAGNET DESIGN

This note is a brief introduction to electromagnet design. It was presented in the Appendix in order to give an idea on how the design of the electromagnet for the electromagnet pumping device were achieved. Electromagnet and applied mathematics books should be consulted for more rigorous understanding of the principle of magnet.

A.1 Maxwell Equations

The basic laws of electricity and magnetism can be summarized by the Maxwell equations:

$$\nabla \cdot \mathbf{D} = \rho \tag{A.1}$$

$$\nabla \cdot \mathbf{B} = 0 \tag{A.2}$$

$$\nabla \times \mathbf{E} = -\frac{\partial \mathbf{B}}{\partial t} \tag{A.3}$$

$$\nabla \times \mathbf{H} = \mathbf{J} + \frac{\partial \mathbf{D}}{\partial t} \tag{A.4}$$

$$\mathbf{D} = \epsilon \mathbf{E} \tag{A.5}$$

$$\mathbf{B} = \mu \mathbf{H} \tag{A.6}$$

[A.1](#) is equivalent to Coulomb's law, which relates the electric field produced by the charge. [A.2](#) states that there are no free magnetic poles, and shows that magnetic field lines never cross each other. [A.3](#) is Faraday's law of induction. [A.4](#) expresses

Ampere's law including the displacement current density as well as the conduction current density.

A.2 Generation of static magnetic field

The basic laws of magnetostatics are

$\nabla \cdot \mathbf{B} = 0$ this is equation (A.2)

$$\nabla \times \mathbf{H} = \mathbf{J} \quad (\text{A.7})$$

the equation (A.7) is the equation (A.4) with no conduction current density included.

considering a closed path C and denote the surface enclosed by the path by S . A surface integral of (A.7) over the area S is

$$\int_S (\nabla \times \mathbf{H}) dS = \int_S \mathbf{J} dS \quad (\text{A.8})$$

By applying Stokes theorem to the left-hand side, next expression is obtained

$$\oint_C \mathbf{H} dS = I, \quad I = \int_S \mathbf{J} dS \quad (\text{A.9})$$

where I is the total current enclosed by the path C . This is the fundamental relation for the magnetic design, which relates the line integral of the magnetic field around a closed path and the total current enclosed by the path. Further it is going to be explain what to do actually in design of magnets, using a simple geometry shown in A-2, with a toroidal core made of iron with a gap g and a coil of n turns and of a current I . BY applying (A.9) to this, following expression relating the magnetic flux density and the current is obtained:

$$\frac{B_0 g}{\mu_0} + \frac{B_i l_i}{\mu_0 \mu_r} = nI \quad (\text{A.10})$$

In the equation (A.10), for simplicity's sake, it is assumed that the magnetic flux density in the gap and the core is constant and given by B_0 and B_i , respectively. l_i is the path length through the core. The permeability of the air gap is virtually the

same as the permeability of vacuum $\mu_0 = 4\pi \times 10^{-7} H.m^{-1}$, while the permeability of magnetic materials, $\mu (= \mu_0 \mu_r)$, depends on B_i . μ_r is the relative permeability, and we often call μ_r just the permeability.

For materials used for magnet cores, the permeability takes its maximum (more than several thousands) at medium fields around 0.3–0.5T, but drops to less than 100 at high fields such as 1.5T. assuming the permeability of magnet core infinite, equation A.10 becomes

$$\frac{B_0 g}{\mu_0} = nI \quad (\text{A.11})$$

This is a basic formula connecting the magnetic flux density B_0 , the gap g and the current I . If the second term of the left-hand side of [?] is not negligible, however, an extra current is required in addition to the current given by [?]. We call this the saturation effects, and degree of saturation term is used.

A.3 Magnetic properties of core materials

We next explain how magnetic materials behave when the magnetic field is varied. A substance is, in general, magnetized when it is placed in a magnetic field. The symbol M usually denotes the magnetization, and M has the dimension of B . Ferromagnetic materials used for magnet cores shows very strong magnetization, and the relation between B (or M) and H is complicated. It is customary, therefore, to use a diagram called the B-H curve shown in A-1, to describe the magnetic properties. considering a toroidal core without gap, uniformly wound by an exciting coil.

starting from the demagnetized state of $M=0$ and $H=0$. With increasing the magnetic field, the magnetization increases and finally saturates to a certain value, which is called the saturation induction. This behavior is described by the magnetization curve denoted by curve 1 in A-1. The permeability, $\mu = B/H$, has its

maximum at medium fields and drastically decreases at high fields. The value of saturation induction is 2.1T for pure iron and somewhat depends on the content of impurities for practical substances.

If the current decreases to zero after the saturation is reached, the B-H relation follows curve 2, instead of the initial curve 1. This is an important property of ferromagnetic materials; the hysteresis effects. At zero current, a certain magnetization M_r still remains at point 1. If the current increases in the reverse direction, the B-H relation crosses the H-axis at point 2 and finally reaches the saturation region in the reverse direction. Point 2 has a particular meaning; a magnetic field $H = -H_c$ is needed to make the magnetization zero. The quantity H_c is called the coercive force, which is an important magnetic property to determine the quality of magnet. If the current comes back to zero and further increases in the normal direction, the B-H curve follows curve 3. This shows that, if a magnet is excited with the sinusoidal wave, its magnetic characteristics basically behave along a closed loop as shown in A-1. It should be noted that the size of the closed loop is dependent on the magnitude of excitation. Fig. A-1 show a magnetic properties of materials sketched by [38].

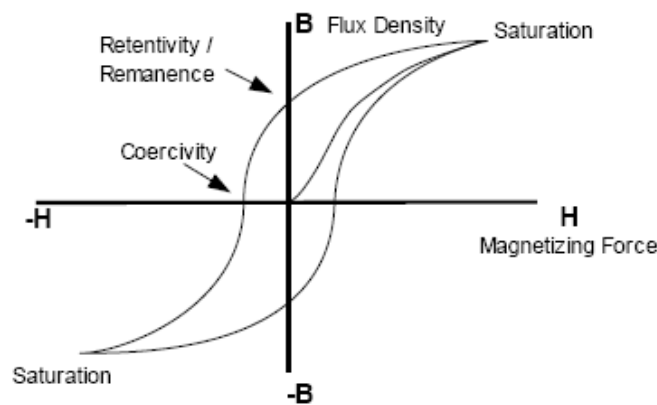


Figure A-1: B-H curve which describes materials magnetic properties

The saturation effect at high fields brings about not only the increase in ampere-turns but also the deterioration of field quality in the gap. When the permeability

of the core can not be considered infinity, the pole face can not be an equi-potential surface. This means the field distribution changes from the ideal one, which is based on the assumption of infinite permeability. This is a deterioration of the field distribution at high fields. In general, the flux density in the pole and the yoke becomes high around the geometrical corners. Therefore, the field strength near a pole edge tends to decrease compared with the central value. When a magnet is used from low fields to high fields, we must be careful of these field deteriorations.

A.4 Remanent field

In section A.3 the hysteresis property of ferromagnetic materials is described , and appearance of non-zero magnetization as well, M_r , at zero current in case of a toroidal core without gap. In this section the behavior of a magnet with a gap will be considered as shown in A-2[38]. When the external current is zero, (A.9) becomes

$$\frac{B_0 g}{\mu_0} + H_i l_i = 0 \quad (\text{A.12})$$

In a rough approximation, the flux density in the core (B_i) can be assumed to be the same as that in the gap (B_o). Then,

$$\frac{B_i g}{\mu_0} + H_i l_i = 0 \quad (\text{A.13})$$

or

$$B_o = \frac{\mu_0 l_i}{g} H_c \quad (\text{A.14})$$

A.14 gives the *remnant field*, which is actually observed in the gap at zero current.

A problem regarding the remanent field is that its field distribution over the transversal aperture is different from that produced by the current with the assumption of infinite permeability. If the magnet operates from very low field to high field. In this case, the core with silicon steel laminations should be made with a low coercive force H_c , to maintain good field qualities at low fields.

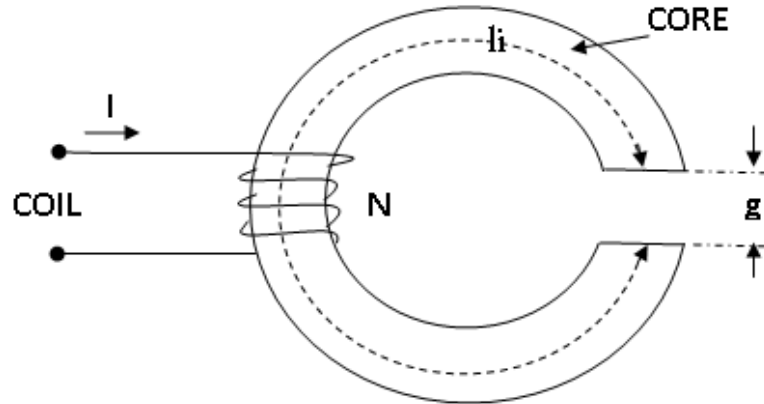


Figure A-2: Toroidal electromagnet with gap

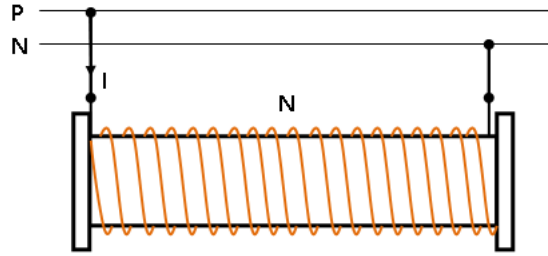
A.5 Eddy current effects

In the case of time varying fields, another problematic phenomenon should be considered. Since core material has a finite resistivity, a current flows in core when the magnetic field is time varying. This is *eddy current*. Two problems arise; one, extra power losses, and second, deterioration of the field distribution in the gap. To reduce eddy currents, we use a laminated core, the thickness of which should be less than 0.35mm

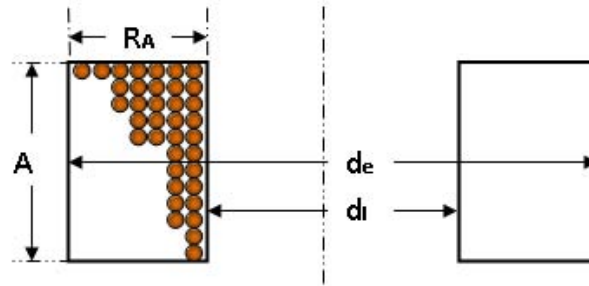
A.6 Connection of coil in derivation

In order to build a derivation connected coil for an electromagnet some considerations should be taking in account. See fig. A-3 [39]

Being the coil subject to a tension of V volts, for coils which being circulated by a intensity current of I amperes it is necessary for the coil resistance to be the same as the Ohm law [40].



(a) Connection diagram



(b) Section view of the coil

Figure A-3: Derivation coil connected

$$V = RI \quad (\text{A.15})$$

In order to calculate the electromagnet dimensions of the coil, some parameters should be fixed to deduce the length of the coil in meters l_m . Designed by N the number of turns of the coil, ρ the conductor resistivity and S_c the conductor section, the coil resistance will be;

$$R = \rho \frac{Nl_m}{S_c} \quad (\text{A.16})$$

substituting this value of R [A.16](#) in the Ohm Law [A.15](#) following value for V is obtained

$$V = \rho \frac{l_m}{S_c} NI \quad (\text{A.17})$$

from equation A.17 the product of NI number of turns per current intensity Θ is the quantity of Amperes-Turns the coil must generate.

thus,

$$V = \rho \frac{l_m}{S_c} \Theta \quad (\text{A.18})$$

From A.18 conductor section can be calculated as,

$$S_c = \rho \frac{l_m}{V} \Theta \quad (\text{A.19})$$

Known the conductor section, conductor dimensions (AWG) can be selected, included the coating film. With the coated Conductor, layers of the coils and turns by layer can be calculated.

$$N_{layers} = \frac{R_a}{d_{coated}} \quad (\text{A.20})$$

where N_{layers} is the number of the layer for the coil, R_a the radial distance of the coil see A-3(b). Now taking the axial distance A, shown in A-3(b) the number of turns by layer is calculated by next expression,

$$N_{turns/layer} = \frac{A}{d_{coated}} \quad (\text{A.21})$$

Known the values from equation A.20 and A.21, the total number of the coil turns N is:

$$N = N_{layers} N_{turns/layer} \quad (\text{A.22})$$

In order the coil can produce the amperes-turns designed it will be necessary that the current move through the wire in a turn with an intensity of,

$$I = \Theta/N \quad (\text{A.23})$$

finally, the current density is calculated by this expression,

$$\delta = I/S_c \tag{A.24}$$

In case the value for density current, calculated in [A.24](#), could be abnormal calculation must be rebuilt from others coils dimensions which results more appropriated.

A.7 Field measurement

The following are the standard methods of measuring the magnetic flux density:

1. Search coil (an application of Faradays law of induction)
2. Hall probe (Hall effect; voltage induced when the current flows through a substance in the presence of the magnetic field)
3. NMR (nuclear magnetic resonance; resonance frequency of microwave selectively absorbed in a substance)

APPENDIX B

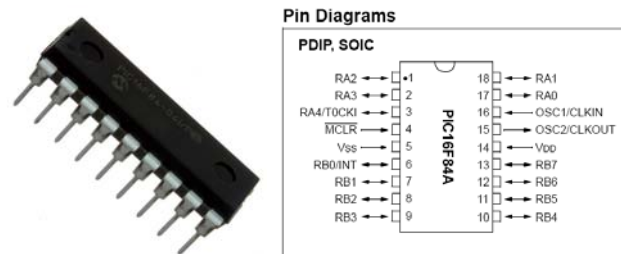
CONTROL CIRCUIT FOR ELECTROMAGNET PUMPING DEVICE

B.1 Control unit

The control unit is a set of electronic devices which is designed to supply the power to the solenoids. Main components and their function are listed on next. Fig. B-4

B.1.1 Components

The Microcontroller, the PIC16F84A Microcontroller belongs to the mid-range family of the PICmicro microcontroller devices. The program memory contains 1K words, which translates to 1024 instructions, since each 14-bit program memory word is the same width as each device instruction. The data memory (RAM) contains 68 bytes. There are also 13 I/O pins that are user-configured on a pin-to-pin basis. Some pins are multiplexed with other device functions. These functions include: external interrupt, change on PORTB interrupt, timer 0 clock input. Fig. B-1



(a) Picture of the component

(b) Paramagnetic

Figure B-1: PIC16F84A Microcontroller

The *optocouplers*, the general purpose of this device consist of a gallium arsenide infrared emitting diode driving a silicon phototransistor in a 6-pin dual in-line package. Applications: dower supply regulators, digital logic inputs and microprocessor inputs. This device is presented in the fig. B-2

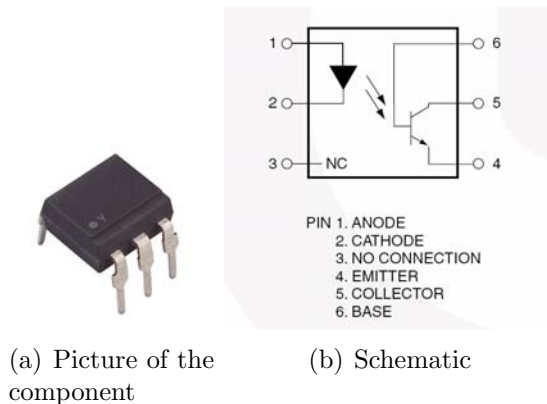


Figure B-2: Optoisolator 4N25

The *mosfet*, fifth Generation HEXFETs from International Rectifier utilize advanced processing techniques to achieve extremely low on-resistance per silicon area. This benefit, combined with the fast switching speed and ruggedized device design that HEXFET Power MOSFETs are well known for, provides the designer with an extremely efficient and reliable device for use in a wide variety of applications. See fig. B-3 for illustration.

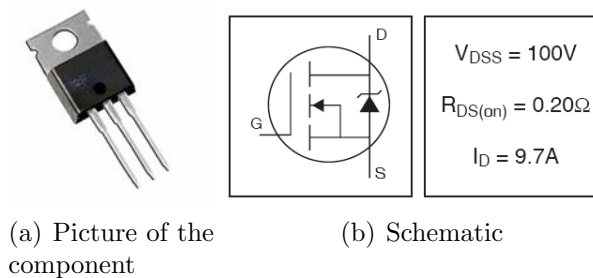


Figure B-3: Power MOSFET IRF520NPbF

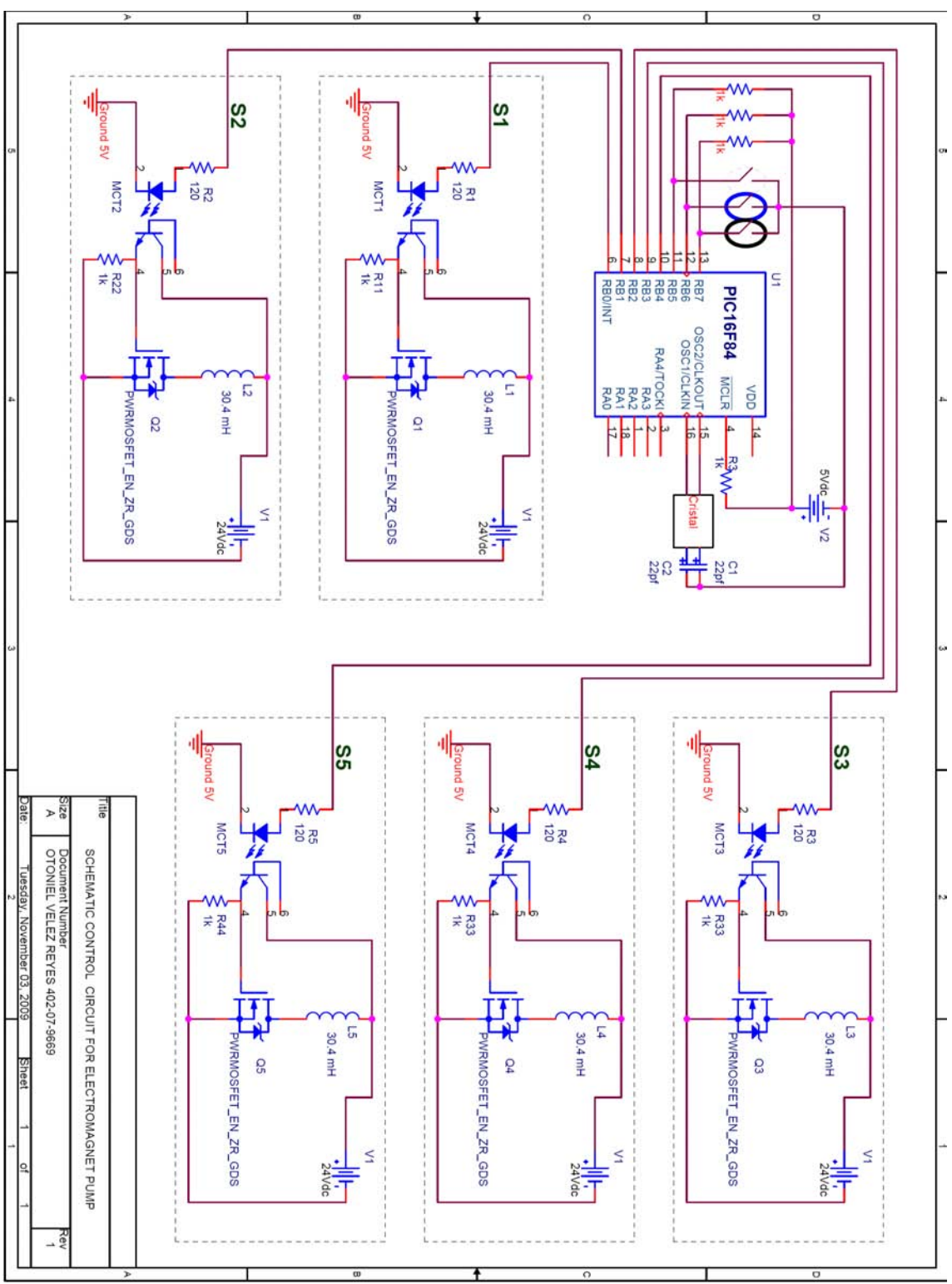


Figure B-4: Schematic control circuit to supply sequenced power to solenoids

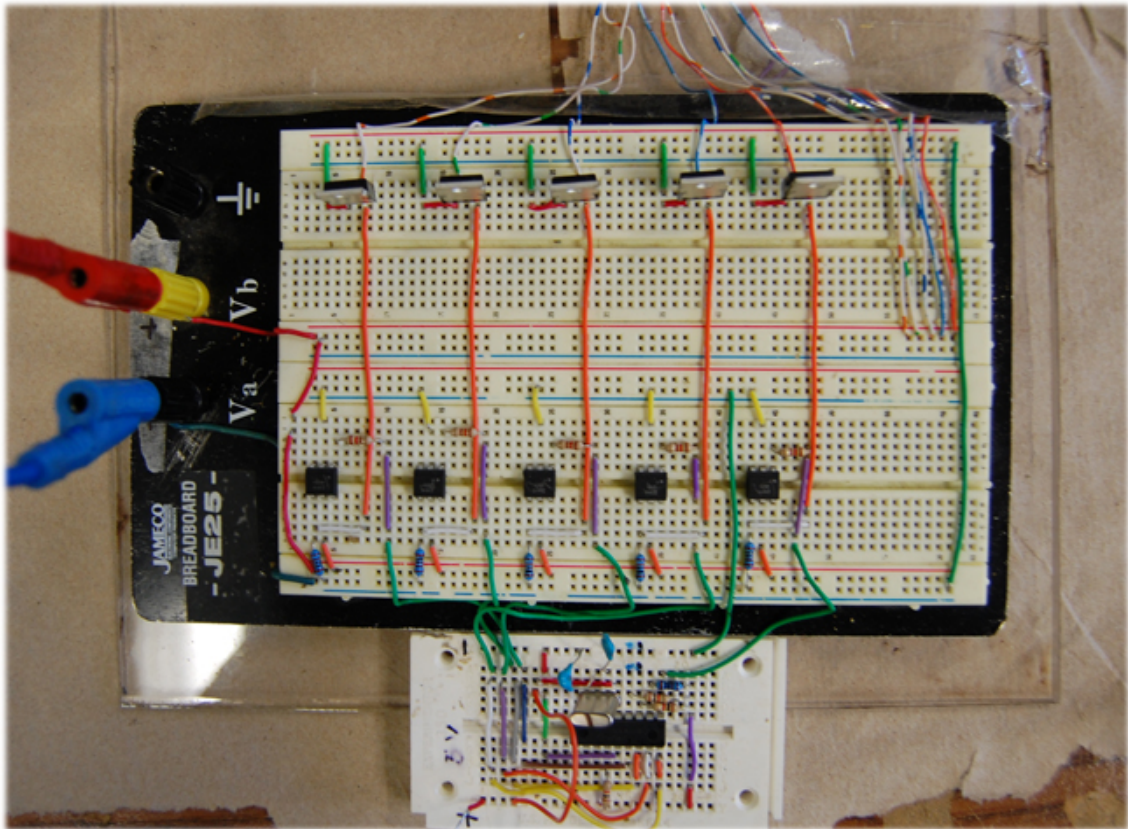


Figure B-5: Control unit circuit to supply sequenced power to solenoids

REFERENCE LIST

- [1] J. Jansen F. Mcknight T. E Roh; Y. L. Love and Phelps T. J. A magnetocaloric pump for microfluidic applications. *IEEE Trans. on nanobioscience*, 3:101–110, Nov 2004.
- [2] S. Shuchi H. Yamaguchi, A. Sumiji and T. Yonemura. Characteristics of thermomagnetic driven motor using magnetic fluid. *Journal of Magnetism and Magnetic Materials*, 272-276:2362–2364, May 2004.
- [3] Q. Li; W. Lian; H. Sun; Y. Xuan. Investigation on operational characteristics of a miniature automatic cooling device. *International Journal of Heat and Mass Transfer*, 51:5033–5039, Jan 2008.
- [4] S. S. Yang O.C. Jeong. Fabrication and test of a thermo-pneumatic micro-pump with a corrugated p+ diaphragm. *Sensors Actuators*, 83:249–255, 2000.
- [5] S. Kluge R. Zengerle, J. Ulrich and M. Ritcher. bi-directional silicon micropump. *Sensors Actuators*, 50:81–86, 1995.
- [6] W. Schomburg R. Rapp and D. Schulz J. Micropump for gases and liquids. *Sensors Actuators*, 40:57–61, 1994.
- [7] S. Richter N. Nguyen, S. Schubert and W. Dotzel. Hybrid assembled micro dosing system using silicon-based micropump/valve and mass flow sensor. *Sensors Actuators*, 69:85–91, 1998.
- [8] A. Olsson P. Enoksson Stemme G. and E. Stemme. Micromachined flat-walled valveless difusser pumps. *Journal of Microelectromechanic*, 6:161–166, March 1994.
- [9] L. S. Tavrow S.F. Bart and M. Mehrengany. Microfavricated electrohydrodynamic pumps. *Sensors Actuators*, 21:193–197, 1997.

- [10] S.S. Lee J. Jang. Theoretical and experimental study of mhd micro-pump. *Sensors Actuators*, 80:84–89, 2000.
- [11] M. C. Murphy L. Huang. fabrication and test of a dc type magneto hydrodynamic micropump. *Microsystem Technology*, 6:235–240, 1995.
- [12] M. Zahn. Magnetic fluid and nanoparticle applications to nanotechnology. *Journal of Nanoparticle*, 3 No. 73:73–78, 2001.
- [13] R.E.Rosenweig. *Ferrohydro-Dynamics*. Dover Publications, Inc. Mineola, New York, first edition, 1997.
- [14] C.N. Chinnasamy K. Hinoda B. Jeyadevan, K. Tohji, and Mn-Zn H. Oka. Ferrite with higher magnetization for temperature sensitive magnetic fluid. *Journal Application of Physics*, 93:170–175, 2003.
- [15] R. A Serway. *Physics for Scientists and Engineers*. James Madison University, 1 edition, 1997.
- [16] A. Molinton. *Basic Electromagnetism and Materials*. Springer Science+Business Media, LLC, first edition, 2007.
- [17] D. J. Griffiths. *Introduction to Electrodynamics*. Prentce-Hall, Inc. Upper Saddle river, New Jersey, third edition, 1999.
- [18] R. Fitzpatric. *Maxwell's Equations and the Principles of Electromagnetism*. Infinity Science Press LLC, Hingham, Massachusetts, first edition, 2008.
- [19] P. Herbert. *Introductory Electromagnetiics*. John Wiley & Sons, Inc., first edition, 1976.
- [20] E.Bermudez. Design and mechanical characterizaiton of a magnetocaloric pump. Master's thesis, University of Puerto Rico at Mayaguez, December 2007.
- [21] M.S Tomar E.Calderon Ortiz, O.Perales Perez P. Voyles. Ferrite nanocrystals for magnetocaloric applications. *Microelectronics Journal*, 40:667–680, Jan 2009.

- [22] H. Stocker H. Lutz W. Benenson, J. W. Harris. *Handbook of Physics*. Springer Science+Business Media, LLC, first edition, 2000.
- [23] C. G.Veinoot. Segregation of losses in single phase induction motors. *Trans AIEE*, 54:1302–2306, 1935.
- [24] E.Warburg. Ann. phys. chem. *Leipzig*, 13:1881, 1881.
- [25] K. Sakatani S. Shuchi and H. Yamaguchi. An application of a binary mixture of magnetic fluid for heat transport devices. *Journal of Magnetism and Magnetic Materials*, 289:257–259, Apr 2004.
- [26] N. Nguyen ; M. Chai. A stepper micropump for ferrofluid driven microfluidic systems. *Micro and Nanosystem*, 1:17–21, Jan 2009.
- [27] M. Lohakan; C. Yensiri; S. Boonsang and C. Pintavirooj. A computational model of ferrofluid flow using maxwell’s equations and navier-stokes equations. *Intl. Conf. on Biomedical and Pharamaceutical Engineering*, 81:467–470, May 2006.
- [28] R. Richter R.Krau, M. Liu B. Reimann and I. Rhberg. Fluid pumped by magnetic surface stress. *New Journal of Physics*, 18:1–11, Jan 2006.
- [29] E. Rlums. and mass transfer processes in temperature sensitive magnetic fluids. *Brazilian Journal of Physics*, 25:112–117, June 1995.
- [30] Q. Li W.Lian, Y. Xuan. Characterization of miniature automatic energy transport devices based on the thermomagnetic effect. *Energy Conversion and Management*, 50:35–42, Oct 2008.
- [31] V.K. Pecharsky K.A. Gschneidner. Magnetocaloric effect and heat capacity in the phase-transition region. *Physical Review*, 59:503–511, Jan 1999.
- [32] K. Hamdache Y. Amirat. Strong solutions to the equations of a ferrofluid flow model. *Jourrnal of mathematical analysis and applications*, 353:271–294, 2008.
- [33] E.Feireisl B. Ducomet. The equations of magnetohydrodynamics. *Math and Physics*, 266:595–629, 2006.

- [34] M. Zahn. *Electromagnetic Field Theory*. Massachusetts Institute of Technology, Department of Electrical Engineering and Computer Science, Cambridge, Ma, first edition, 1990.
- [35] M.Riccetti. Optimization and characterization of a magnetocaloric pump using ferrofluids. Master's thesis, University of Puerto Rico at Mayaguez, May 2009.
- [36] I. Boldea and S.A. Nasar. *The induction machine handbook*. Boca raton New York, first edition, 2001.
- [37] Wikipedia. American wire gauge. *wikipedia.org*, N/D:1–3, 2009.
- [38] M.Kihara. An introduction to electromagnet design. June 2000.
- [39] V. Valkenburgh. *Basic Electricity*. Nooger and Neville, Inc., first edition, 1974.
- [40] E. Afha. *Electricity Volume I*. S.A Barcelona, Inc., first edition, 1976.